REPUBLIC OF TURKEY
ACIBADEM MEHMET ALİ AYDINLAR UNIVERSITY
INSTITUTE OF HEALTH SCIENCES

FUNCTIONAL ANALYSIS OF AN *IRIDOVIRUS* KINASE GENE ORF 389L

ÖMER FARUK TAŞTAN

MASTER THESIS

DEPARTMENT of MEDICAL BIOTECHNOLOGY

SUPERVISOR

Prof. Dr. İkbal Agah İnce

SECOND SUPERVISOR

Assist. Prof. Dr. Arzu Özgen

İSTANBUL-2019

REPUBLIC OF TURKEY
ACIBADEM MEHMET ALİ AYDINLAR UNIVERSITY
INSTITUTE OF HEALTH SCIENCES

FUNCTIONAL ANALYSIS OF AN *IRIDOVIRUS* KINASE GENE ORF 389L

ÖMER FARUK TAŞTAN

MASTER THESIS

DEPARTMENT of MEDICAL BIOTECHNOLOGY

SUPERVISOR

Prof. Dr. İkbal Agah İnce

SECOND SUPERVISOR

Assist. Prof. Dr. Arzu Özgen

İSTANBUL-2019

Department:	Institute of Health Sciences
Program:	Medical Biotechnology
Thesis Title:	Functional Analysis of an *iridovirus* kinase gene ORF 389L
Student's name and Surname:	Ömer Faruk Taştan
Date of Defance:	02/ 08/2019

This is to certify that Ihave examined this copy of master thesis. I have found that she/he prepared after fulfilling requirements specifed in the associated legislalations before the final examining committee whose signatures are below.

Jury president	Prof. Dr. Tanıl Kocagöz Acıbadem Mehmet Ali Aydınlar University
Supervisor of the thesis	Prof. Dr. İkbal Agah İnce Acıbadem Mehmet Ali Aydınlar University
Jury Member	Assist. Prof. Dr. Arzu Özgen İstanbul Gelişim University
Jury Member	Assoc. Prof. Dr. Ömer Faruk Bayrak Yeditepe University
Jury Member	Prof. Dr. Sesin Kocagöz Acıbadem Mehmet Ali Aydınlar University

DECLARATION

I hereby declare that this thesis has been written by me based on data obtained in line with the scientific rules and ethical principles of responsible conduct of research. All information, data, comments and analyses have been collected and processed using a scientific, academic writing style, and all literature used has been duly shown by referring to the original sources in accordance with publication ethics. I also announce and emphasize that I have not violated any rules secured by patents and copyrights during the conduct of this research and the writing of this thesis.02.08.2019

Ömer Faruk Taştan

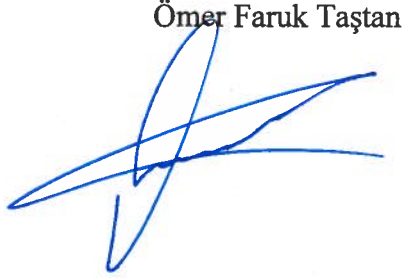

ACKNOWLEDGEMENTS

Firstly, I would like to thank Acıbadem Mehmet Ali Aydinlar University for scholarship covering my master study and my supervisor Dr. İkbal Agah İnce, for his patient guidance, enthusiastic encouragement and useful critiques of this research work. I would also like to thank my co-supervisor Dr. Arzu Özgen for all her support, especially during the laboratory work. My grateful thanks are also extended to Dr. Orhan Özcan for his help with the bioinformatics data analysis. I would also like to extend my thanks to Dr. Ayca İlter Akülke for her help in teaching me several molecular biology methods, especially cell culture experiments.

I would like to offer special thanks to my colleague Fatma Pınar and the research laboratory members of the laboratory of basic medical sciences for their help during my master studies.

Finally, I would like to thank my family and Burcu Taluğ who have been with me throughout this thesis and who have always supported me. I am grateful for everything they have done for me.

LIST OF CONTENTS

Page

LIST OF SYMBOLS AND ABBREVIATIONS

FAO: Food and Agriculture Organization of the United Nations

NPV: *Heliothis nucleo* polyhedrosis virus

IIV: Invertebrate Iridescent Virus

PCD: Programmed cell death

ATP: Adenin Triphosphate

ORF: Open Reading Frames

***iap*:** Inhibitor of Apoptosis

BIR: Baculoviral *iap* Repeat

Sf: *Spodoptera frugiperda*

SPC-BM-36: Silkworm (*Bombyx mori*) 36

dsDNA: Double-strand DNA

ICTV: International Committee on Taxonomy of Viruses

NCLDV: Nucleocytoplasmic Large dsDNA Viruses

CIV: Chilo Iridescent Virus

ER: Endoplasmic Reticulum

GPI: Glycophosphatidylinositol

$MgCl_2$: magnesium chloride

EDTA: Ethylenediaminetetraacetic acid

vsiRNAs: Viral Small Interfering RNAs

AGO2: Argonaute

RNAi: RNA interference

miRNA: microRNA

FV3: Frog Virus

CAM: Cell Adhesion Molecule

IE: Immediate Early

DE: Delayed Early

L: Late

NTP: Nucleotide Triphophatase

TNF: Tumor Necrosis Factor

CARD: Caspase Recruitment Domain

DED: Death Effector Domains

DISC: Death-Inducing Signal Complex

JNK: c-Jun N-terminal kinase

Apaf-1: Apoptotic protease activating factor 1

TUNEL: Terminal Deoxynucleotidyl Transferase dUTP Nick End Labeling

k-DA: kilodalton

K/o: Knock-out

O/e: Over-expressed

FBS: Fetal Bovine Serum

eGFP: Enhanced Green Fluorescent Protein

***mcp*:** Major Capsid Protein

K/r: Knock-Out Recombination

O/r: Over-express Recombination

PCR: Polymerase Chain Reaction

ADB: Agarose Dissolving Buffer

OD: Optical Density

TCID: Tissue Culture Infectious Dose

MDV: Marek's Disease Virus

LIST OF FIGURES

Page

LIST OF TABLES

Page

SUMMARY

Programmed cell death (apoptosis) is a key host response to virus infection. Invertebrate Iridescent Virus *6* (IIV-6) is the type species of the genus *Iridovirus*, a member of the Iridoviridae family, and the virions contain a single linear dsDNA molecule. It was previously reported that IIV-6 gene ORF 389L encoding protein, which is serine-threonine protein kinase, can induce apoptosis in insect cells. They showed that protein of 389L gene induced apoptosis in the different insect cell line. However, the apoptotic role of 389L gene was not assigned in the genomic level. We have generated two types of recombinant IIV-6 to evaluate whether the apoptotic interaction of 389L gene has changed at the genomic level. In our study, ORF 389L (iridoptin) knocked-out and ORF 389L over-expressing IIV-6 using a strong IIV-6 promotor (major capsid protein gene promotor of IIV-6) were generated via the homologous recombination method. The plaque assay method was used to purify the recombinant virus from the wild-type (w/t) virus via visualizing eGFP signal under a Zeiss AX10 microscope (Carl Zeiss, USA). After the seven plaque assay purification experiments, two types of recombinant viruses were generated, which was confirmed through the PCR method with observing recombinant DNA regions with suitable primers. Furthermore, one-growth assay studies showed that, in comparison to ORF 389L knocked-out and wild type IIV-6, ORF 389L over-expressed IIV-6, has a noticeably higher viral titer after 48 hours. Therefore, it can be suggested that 389L gene both affects the replication of IIV-6 as well as triggers the release of higher viral progeny cell to cell. Consequently, working with a model dsDNA virus is crucial to the understanding of these fundamental mechanisms which can be used as an anti-viral drug for serious viruses such as the large DNA smallpox virus.

Key Words: dsDNA virus, IIV6, Invertebrate, Kinase, Apoptosis, Insect, Live Imaging

ÖZET

Iridovirus Kinaz Geni Olan ORF 389l'nin Fonksiyonel Analizi

Programlanmış hücre ölümü (apoptoz), virus enfeksiyonuna karşı hücrelerin savunma mekanizmasıdır. Invertebrate Iridescent Virus 6 (IIV-6), Iridoviridae familyasının bir üyesi olan *Iridovirüs* cinsinin türüdür ve virionları tek bir lineer dsDNA molekülü içerir. Chitnis ve arkdaşları tarafından 2011 yılında serin-treonin protein kinaz geni olan 389L'yi kodlayan proteinin böcek hücrelerinde apoptozu indüklediği rapor edilmiştir. Fakat 389L geninin apoptotik rolü genomik seviyede belirlenmemiştir. Bu tez çalışmasında 389L geninin apoptotik etkileşiminin genomik düzeyde değişimini belirlemek üzere iki tip rekombinant IIV-6 geliştirilmistir. Çalışmamızda 389L (iridoptin) ORF'si hem genomdan silindi ve hem de güçlü bir IIV-6 promotörü (IIV-6'in major kapsid protein gen promotörü) kullanarak 389L genini aşırı ifade eden IIV-6, homolog rekombinasyon yöntemi ile üretildi. İnfeksiyoz ünitenin belirlenmesi ile Zeiss AX10 mikroskobu (Carl Zeiss, ABD) altında eGFP sinyalleri gözlemlenerek rekombinant virus, yabani tip (w/t) virüsten saflaştırıldı. Yedi plak testi saflaştırma deneyinden sonra, PZR yöntemi ile doğrulanan iki tip saf rekombinant virüs üretildi. Ayrıca, virüs büyüme eğrisinin oluşturulma çalışması, 389L nakavt IIV-6, yabani tip IIV6 ile karşılaştırıldığında, IIV6'i aşırı ifade eden ORF 389L'nin 48 saat sonra açıkça daha yüksek viral titreye sahip olduğunu göstermiştir. Sonuç olarak, bir model dsDNA (çift zincirli) virusü ile çalışmak, büyük DNA çiçek virusü gibi ciddi virusler için anti-viral bir ilaç olarak kullanılabilecek bu temel mekanizmaların anlaşılması için çok önemlidir.

Anahtar Sözcükler: dsDNA Virüsü, IIV6, Omurgasızlar, Kinaz, Apoptoz, Böcekler, Görüntüleme

1. AIM OF STUDY

Insects comprise a large proportion of all biodiversity on the planet. So much so, that over half of the estimated 1.5 million organism species described are classified as insects. Insects can be found in all habitats; jungles, oceans, swamps, and deserts, as well as in extreme environments such as crude petroleum pools or volcanoes (1). Insect organisms have a very close relationship with humans and with their environment. This relationship can be helpful or harmful. Several insect species are predators, or parasitoids of various harmful pests, while other insects are pollinator and produce valuable products such as honey and silk. Even though less than 50 per cent of the total number of insects is considered a pest, they can still be a serious menace to agricultural crops. Since insects can lead to serious damage, several control methods have been developed to prevent them from doing damage, and one of the most efficient methods is known as the self-control method. The beauty of the self-control method is that it directly affects the targeted insects while doing no harm to the environment. Therefore, the preferred way of minimizing the harmful insects can do to an environment is the biological self-control method, using biological control agents. There are several insect infecting agents including viruses, fungi, bacteria, protists and nematodes (2). Ever since the discovery of the insect-fighting viruses' virulence and the way they will only target one insect, using viruses as an insecticide has been researched heavily. The first time this method was officially used was when the US Food and Drug Administration approved the use of the Heliothis nucleopolyhedrosis virus (NPV) against *Heliothis* genus on cotton in the 1970s. In addition, NPV has been extensively tested on corn, tobacco and truck crops infected by *Heliothis* genus (3). Following this study, several field trials were done on using viruses as candidates for biological pest control. One of the species studied is the Invertebrate Iridescent Virus Type 6 (IIV-6) which belongs to the family Irodivirids, under the *Iridovirus* genus. IIV-6 can be used as a potential biological control agent to control invasive insects that can harm agricultural crops like tea, nuts and cotton. IIV-6 usually causes an inapparent (covert) infection that reduces host fitness. Marina et al showed that IIV-6 infection leads to a 34% decrease in the net reproductive rate of infected mosquitoes. Furthermore, in comparison to other insects, the high killing capacity of IIV-6 allows it to become a

potential biological pest agent. However, its slow mortality rate function makes it rare to use (4,5). For instance, Jenkins et al showed that IIV-6 causes infection in *Phyllophaga vandinei* Smyth (Coleoptera: Scarabaeidae), but the mortality rates of an infection were determined to be ~30% (4) and Yu et al observed 70% mortality in the cotton boll weevil (*Anthonomus grandis*) (6).

Programmed cell death (PCD) is the death of a cell-mediated by an intracellular program, and apoptosis is one of the forms of PCD. Apoptosis is typically characterized by chromatin condensation, cell and nuclear shrinkage, cytoplasmic blebbing and caspase activation. Apoptosis is the main protective defence mechanism of host cells since it prevents the replication, propagation or persistence of viruses. However, over time viruses have evolved with their host, learning to modulate apoptosis. In other words, viruses sometimes actually induce apoptosis to release progeny particles or inhibit apoptosis to allow viral replication and propagation (7). Through modulating the regulation of the apoptosis mechanism, viruses can release a new generation of progeny virus particles and maintain viral persistence (8). Of the apoptotic process proteins, protein kinases play a pivotal role in each step of the apoptosis. Protein kinases catalyze the transfer of a phosphate group from a nucleoside triphosphate (usually ATP) to another protein, and this phosphorylation usually leads to changes in the enzymatic activity of another protein, mostly its cellular localization or interaction with other proteins. Ever since the IIV-6 genome was sequenced by Jacob et al (9), the potential apoptosis inducing or anti-apoptotic open reading frames (ORFs) can be easily predicted. For instance, İnce et al determined that three gene (157L, 193R and 332L) of IIV-6 have homology to the genes that inhibit apoptosis *(iap)* in baculovirus. They also noticed that these genes include C-terminal RING domains, although only the 193R gene contains a baculoviral *iap* repeat (BIR) domain. Furthermore, they showed the role of the 193R gene inhibiting apoptosis in the Sf21 and SPC-BM-36 cell lines (7). More recently, Chitnis et al detected the signature sequences of ATP binding and serine-threonine kinase in the 389L gene of IIV-6. They also showed that a serine-threonine kinase protein of IIV-6, 389L (named *iridoptin*), induces apoptosis in boll weevil cells and budworm (10). To understand the effect of 389L gene on the pathogenesis of IIV-6, including apoptosis, one of the most reliable

methods is to generate a recombinant virus via the homolog recombination method (11).

Double-strand DNA (dsDNA) viruses can be separated into three groups: (i) small size DNA (10 kb) virus, (ii) medium size DNA virus (35 kb), and large size DNA virus (150 to 250 kb). dsDNA viruses share common features: replication strategy, viral gene expression, apoptotic interaction etc. These similarities are milestones that can illuminate the molecular mechanisms of dsDNA viruses. For instance, in the past, research on bacteriophages has made a significant contribution to prokaryotic molecular biology; similarly, research on animal viruses has contributed to eukaryotic molecular biology. In addition, IIV-6 has large linear double-stranded DNA and the DNA terminally redundant and circularly permuted. Further studies about IIV-6 will increase the knowledge about dsDNA virus-host interaction.

This study aims to investigate the role of 389L gene. In order to investigate the infective role of 389L gene, ORF 389L was stably knocked-out (k/o) and overexpressed (o/e). Furthermore, the growth rate of w/t, 389L k/o and 389L o/e IIV-6 generations were compared using the one-step growth curve assay method (12).

2. INTRODUCTION

2.1 Insect Viruses

As expected, insect viruses are present in most of the major viral taxa. Since beneficial (pollination etc.) insects (such as honey bees and silkworms) have a potential mechanism to protect themselves from viruses (13, 14), insect viruses could be used for the management of harmful insects in agriculture (15) or to prevent spreading of insects that carry viruses that are harmful to humans, animals and plants (16).

Virus classification is subject to ongoing debate and proposals. To reduce these debates, a first attempt to determine a universal taxonomic scheme for virus classification was carried out by a group of scientists who met in Moscow in 1966. They are known as the International Committee on Taxonomy of Viruses (ICTV). The ICTV database classifies a virus according to virion size and shape, the presence of an envelope, GC content of the genome, genome organization and replication strategy of the virus, lipid and carbohydrate content etc. Virus classifications are constantly being updated and shared with the world through published reports. Currently, there are 8 virus orders and 125 virus families in the ICTV database. Up to now, 16 virus families have been isolated from insects. These virus families were created by grouping large numbers of insects together based on certain characteristics (17) (Table 2.1).

Table 2.1 Insect Viruses and Their Some Features.

Family	Insect-infecting genera	Genome	Virion shape and diameter
Baculoviridae	*Alphabaculovirus* *Betabaculovirus* *Gammabaculovirus* *Deltabaculovirus*	dsDNA circular 80-180 kbp	Rod-shaped; 30-60 nm x 250-300 nm

Poxviridae	*Alphaentomopoxvirus* *Betaentomopoxvirus* *Gammaentomopoxvirus*	dsDNA linear 250 + 250 kbp	Ovoid or Brick-shaped; 160-250 nm x 300-470 nm
Reoviridae	*Cypovirus* *Idnovirus*	dsRNA 10 segments	Icosahedral 80 nm
Iridovirids	*Iridovirus* *Chloriridovirus*	dsDNA 140-210 kbp	Icosahedral 120-180 nm
Polydnaviruses	*Bracovirus* *Icnovirus*	dsDNA 150-250 kbp	Irregular/prolate ellipsoid > 200 nm in length
Ascoviridae	*Ascovirus*	dsDNA circular 120-180 kbp	Allantoid, reinform 130 nm x 200-400 nm
Parvoviridae	*Densovirus* *Iteravirus* *Brevidensovirus* *Pufudensovirus*	ssDNA 5-6 kbp	Icosahedral 18-26 nm
Birnaviridae	*Entomobirnavirus*	dsRNA 2 segments	Icosahedral 60 nm
Rhabdoviridae	Unassigned	ssRNA - ; 11-15 kb	Bullet- shaped 45x100 nm - 100-430 nm
Dicistroviridae	*Cripavirus*	ssRNA + ; 9-10 kb	Icosahedral 30 nm
Iflaviridae	*Iflavirus*	ssRNA + ; 8.5-9.5 kb	Icosahedral 30 nm
Caliciviridae	Unassigned	ssRNA + ; 7.5-8.5 kb	Icosahedral 35-40 nm
Tetraviridae	*Betatetravirus* *Omegatetravirus*	ssRNA + ; 1-2 segments 6.5-8 kb	Icosahedral 40 nm
Nodaviridae	*Alphanodavirus*	ssRNA + ; 2 segments 4.5 kb	Icosahedral 32-33 nm
Metaviridae	*Metavirus* *Errantivirus*	ssRNA + ; 4-10 kb	Irregular ~ 100 nm

Pseudoviridae	*Pseudovirus* *Hemivirus*	ssRNA + ; 5-10 kb	Irregular; round to ovoid 30-40 nm

Ref (17): Christian PD, Possee RD. Insect Viruses. First Edition, eLS. 2008

Iridoviruses belong to the Iridoviridae family and infect a large number of insects. They were featured in a broad title in the 10th ICTV report published in 2017 (18). Members of the Iridoviridae family are nucleocytoplasmic large dsDNA viruses (NCLDVs). The family is divided into two subfamilies (Betairidovirinae and Alphairidovirinae) and five genera (*Ranavirus*, *Megalocytivirus*, *Lymphocystivirus*, *Chloriridovirus* and *Iridovirus*). *Ranavirus*, *Megalocytivirus*, *Lymphocystivirus* infect cold-blooded vertebrates such as reptiles, amphibians and fish, whereas *Chloriridovirus* and *Iridovirus* mainly infect invertebrates such as crustaceans and insects. According to the current classification scheme, the genus *Iridovirus* uses a name that is consistent with the host species of initial isolation, and a type number relating to the chronological order of discovery: Invertebrate iridescent virus 1 (IIV-1), was the first IIV species that was discovered and isolated from the soil-dwelling European crane fly *Tipula paludosa* (19). Recently, the family name Iridoviridae has been replaced by ” Iridovirids” to avoid confusion between members of the genus and family (20). The Iridovirids genera are distinguished based on host preference, virion particle size, genomic GC content, the amino acid sequences of the major capsid protein and the presence of DNA methyltransferase genes (21). While current phylogenetic analysis is based on amino acid sequencing of the major capsid protein, complete genome sequencing offers more detailed data for an advanced phylogenetic classification (20). However, there is still not enough genome sequencing data on iridovirids. Within the genus, *Iridovirus*, only IIV-1 (19) and IIV-6 (22), also referred to as Chilo Iridescent Virus (CIV), have been sequenced (20).

2.2 Introduction to IIV-6

IIV-6 is an NCLDV and a member of the Iridovirids under the *Iridovirus* genus. IIV-6 is also named Chilo Iridescent Virus (CIV), and the original form of the virus was

isolated from the diseased larva of the rise stem borer, *Chilo suppresalis* (Lepidoptera; Pyralidae) in Japan (22). In case of infection with IIV-6, the virion particle massively proliferates in the host cell cytoplasm, leading infected insects to display an iridescent colour ranging from green to violet, leading to IIV-6 being also known as the iridescent virus.

2.2.1 Morphological Characteristics of IIV-6

The IIV-6 virus particle includes three main components: an outer capsid layer, an intermediate lipid membrane and a nucleocytoplasmic dsDNA genome (Figure 2.1). Though naked virions of IIV-6 can reach up to 185 nm in diameter when observed using CryoEM and 3D image construction, the size of IIV-6 was determined to be between 120-130 nm (23,24).

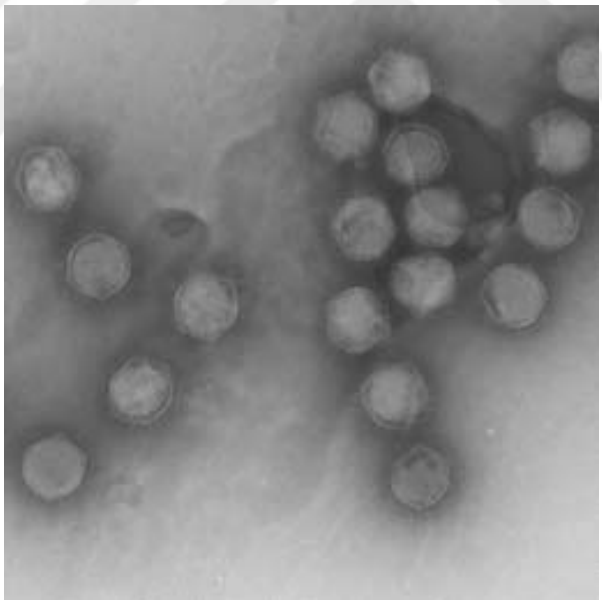

Figure 2.1 Electron micrograph of IIV-6.
Ref (25): Nalçacıoğlu R, Ince IA, Demirbağ Z. The biology of Chilo iridescent virus. Virol Sin. 2009;24(4):285–94.

The IIV-6 lipid membrane is predominantly composed of glycophosphatidylinositol (GPI). The IIV-6 lipid membrane differs in appearance from their host cell, and interestingly it is analogous with the host's endoplasmic reticulum (ER) membrane.

This means that IIV-6 membrane is not likely derived from the host cell membrane, as it can be derived from the host's ER membrane (20). In addition, IIV-6's outer lipid GPI acts as a protein anchor, with proteins attaching via the C-terminal (26). The GPI anchored proteins can act as extracellular receptors or cell surface antigen/cell adhesion molecules, but their most important function is providing stable anchoring to IIV-6 to protect extracellular proteases and lipases (26).

2.2.2 Stability of IIV-6

The stability and sensitivity of IIV-6 were measured by using different conditions (27–29) and various chemicals (27). IIV-6 is stable in water (28) and moist soil conditions, but not stable above 55 °C, in ultraviolet radiation, in solar UV light (29), in different pHs (28) and in non-sterile conditions.

In addition, Reyes et al. (30) showed that IIV-6 is very sensitive to dry soil, but the moisture level doesn't affect the stability of IIV-6. Also, sterile soil appeared to decrease IIV-6 infectivity and stability. In damp soil, IIV-6 was found to have a half-life of 4.9 days in non-sterile soil, 6.3 days in sterilized soil and 12.9 days in the control virus suspensions (all held at 25°C in a microcentrifuge tube) (Figure 2.2)

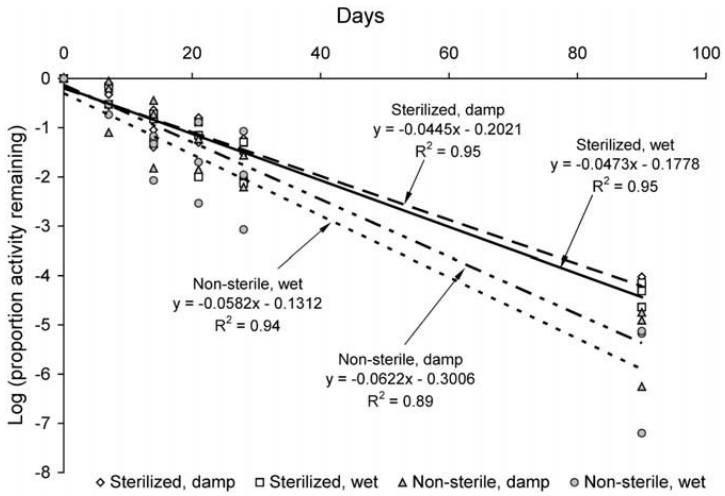

Figure 2.2 Activity results of IIV-6 from Galleria mellonella insect bioassay. The activity of IIV-6 present in damp (17% moisture) and wet (37% moisture) sterilized and non-sterile soil following 90 days at 25◦C.

Ref (30): Reyes A, Christian P, Valle J, Williams T. Persistence of Invertebrate iridescent virus 6 in soil. BioControl. 2004;49(4):433–40.

IIV-6 is thermolabile and when heating IIV-6 to 70 °C for 60 min or 80 °C for 30 min, viral activity rapidly decreased by approximately four logs. In addition, 36 hours of exposure to solar UV light leads to a complete loss of viral infectivity (29). IIV-6 was found to be sensitive to chloroform, ether, sodium deoxycholate, 1 and 0.1% SDS, 1% Triton-x-100, 70% ethanol and 70% methanol. However, Tween-80, proteinase-K, lipase, magnesium chloride ($MgCl_2$), ethylenediaminetetraacetic acid (EDTA) and other proteinases did not affect the stability and infectivity of IIV-6 (27).

2.2.3 IIV-6 Hosts

IIV-6 has more than 100 natural hosts, belonging to six orders; Coleoptera, Hemiptera, Orthoptera, Lepidoptera, Hymenoptera and Diptera. Literature shows that IIV-6 can be propagated in 17 different cell line lines: *Aedes albopictus* (31), *Aedes aegypti* (31), *Anticarsia gemmatalis* (BCIRL-AG-AM) (31), Drosophila line 2 (DL2) (31), Drosophila line 1 (DR1) (31), *Helicoverpa zea* (BCIRL-Hz-AM1) (31), *Heliothis virescens* (BCIRL-HV-AM1) (31), *Pieris rapae* (PR-5) (31), *Plutella xylostella* (BCIRL-PX2-HNV3) (31), *Spodoptera frugiperda* line 21 (Sf21) (31), *Spodoptera frugiperda* line 9 (Sf9) (31) and *Trichoplusia ni* (TN-CL1) (31), *Bemisia tabaci* (whitefly) (32), *Circulifer tenellus* (leafhopper) (33), *Ceraeochrysa cubana* (lacewing) (33), *Diaprepes abbreviates* (root weevil) (34), *Anthonomus grandis* (boll weevil) (6). Also, even though IIV-6 can infect *Ostrinia nubilalis* larvae in certain tissues and cells, cell culture lines of this larva derived from hemocytes were barely infected with IIV-6 (35).

2.2.4 Pathology of IIV-6

Iridescent colouring in the infected host is the clearest sign of IIV-6 disease. Due to the presence of crystalline arrays of virus particles in the infected host cytoplasm, an iridescent colour appears. However, covert infections of IIV-6 are more common,

affecting reproductive activity and longevity of the infected hosts. Unusually, patent infections of IIV-6 are lethal for the majority of the host (36).

dsRNA produced by DNA and RNA viruses is the main signal that triggers an innate immune response in the infected host's immune system. Molecular response pathways are different between vertebrates and invertebrates. In vertebrates, viral dsRNA is converted into viral small interfering RNAs (vsiRNAs) by Dicer-2 (Dcr-2). Then vsiRNAs are fused to Argonaute (AGO2) in the RNA-induced silencing complex (RISC) to cleave viral target RNAs. All molecular antiviral response based on RNA is denominated as RNA interference (RNAi) (Figure 2.3).

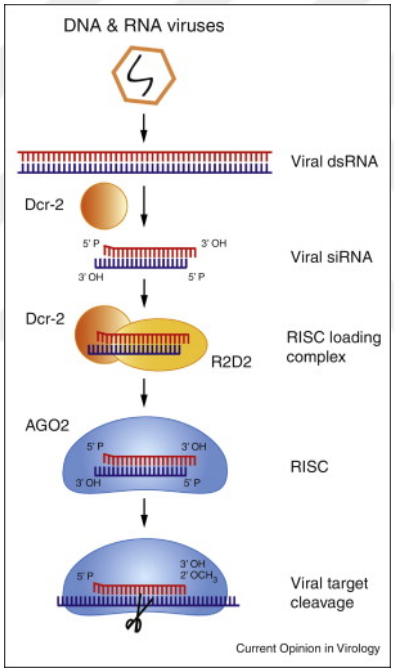

Figure 2.3 Schematic representation of the antiviral RNAi pathway.
Ref (37): Bronkhorst AW, van Rij RP. The long and short of antiviral defense: small RNA-based immunity in insects. Curr Opin Virol. 2014;7:19–28.

2.2.5 Genomic Features, Replication and Transcription of IIV-6

The IIV-6 genome comprises of 212,482 bp DNA with 28,63% GC content which is circularly permuted and terminally redundant (9,37). Although there are 468 overlapping and non-overlapping ORF in the IIV-6 genome, the coding capacity of the

genome is 215 ORF (Figure 2.4) (20). In addition, even though IIV-6 mRNAs lack introns and poly(A) tails (38), some studies suggest that there are microRNAs (miRNA) acting as IIV-6 transcripts that may modulate viral gene expression (39).

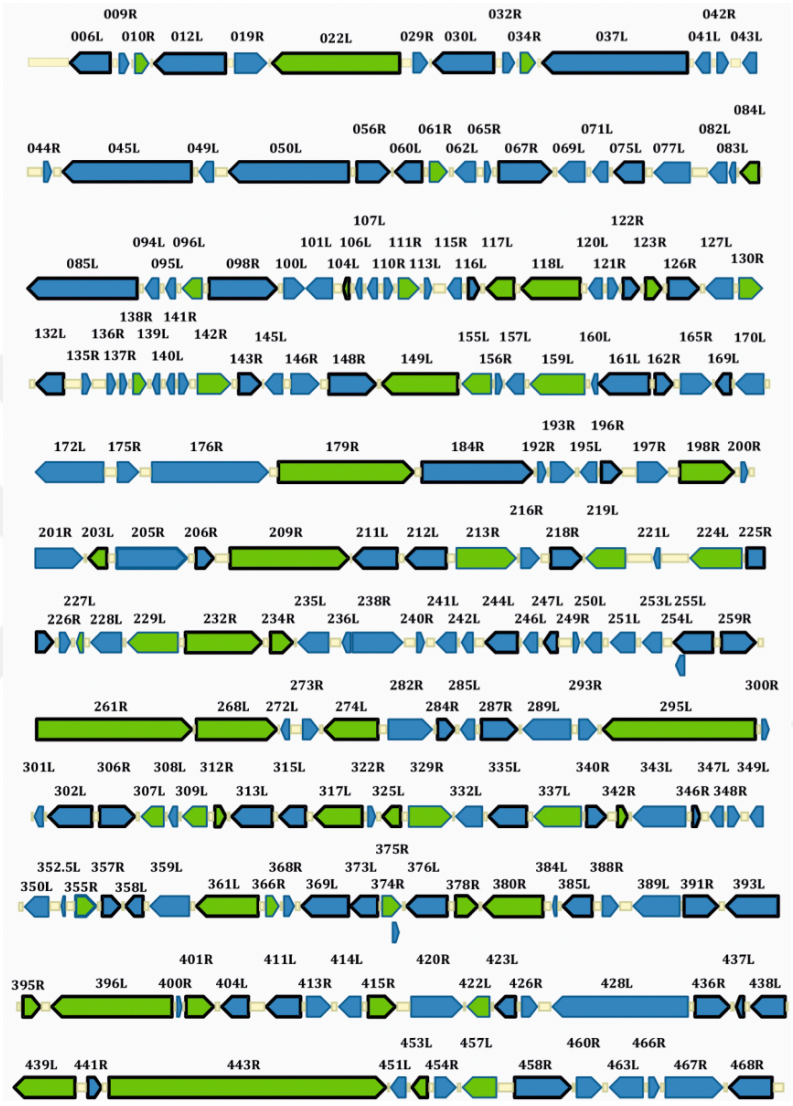

Figure 2.4 Virion and viral proteins of IIV-6 in infected cells identified through mass spectrometry. Known virion proteins are indicated by green arrows, and proteins detected in infected cells are indicated by black arrows.
Ref (40): Ince IA, Boeren S, van Oers MM, Vlak JM. Temporal proteomic analysis and label-free quantification of viral proteins of an invertebrate iridovirus. J Gen Virol. 2015;96(1):196–205.

Genome replication and transcription of IIV-6 is best characterized by the Frog Virus (FV3), which belongs to the genus of *Ranavirus* under the iridovirids, and has served as a model to understand the genomic replication of IIV-6. Replication in Iridovirids

occurs in two stages (41): Before the replication, the virus attaches to a cell surface receptor. In IIV-6, 096L gene is suggested to be a cell adhesion molecule (CAM) that assists the progress of the attachment to the cell surface (20). Following the attachment of the virus, the virus enters the cell cytoplasm via receptor-mediated endocytosis. After penetration, viral DNA is transported to the cell nucleus, after which viral replication begins. To understand transcription time, three types of viral transcript were determined: immediate early (IE) (0 and 2 h.p.i), delayed early (DE) (2 to 4 h.p.i) and late (L) (after 6 h.p.i) (42–44). IE and DE transcripts are synthesized in the nucleus, whereas L transcripts are synthesized in the cytoplasm. Early transcripts are crucial for replication and expression of late genes, and late transcripts are the main components of the virion (42). After the first replication, a second replication occurs in the cytoplasm, where concatemers of the virion are formed, which are up to ten times larger than the viral genome. Late transcripts are synthesized by host RNA polymerase which is modified by a virus or by a viral polymerase that has not yet been characterized. The progeny virions are released from the cell by either budding or a type of cell lysis that has not been identified, or they accumulate in the cytoplasm in large paracrystalline arrays.

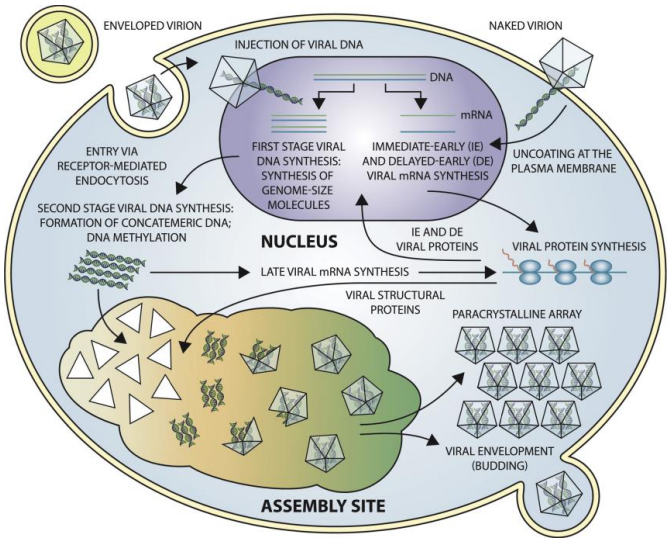

Figure 2.5 Representation of Iridovirid Replication.
Ref (18): Chinchar VG, Hick P, Ince IA, Jancovich JK, Marschang R, Qin Q,. ICTV virus taxonomy profile: Iridoviridae. J Gen Virol. 2017;98(5):890–1.

2.2.6 Total Transcript and Proteins of IIV-6

A study showed that a total of 137 viral transcripts were expressed as 38 IE, 34 DE and 65 L gene transcripts. 54 proteins of IIV-6 have been identified (40), but due to the lacking similarity to annotated protein, 39 protein roles cannot be predicted, and these proteins should be investigated further.

Possible functions of 15 proteins were assigned as carboxy-terminal domain phosphatase, 355R; cathepsin, 361L; DNA binding protein, 401R; DNA polymerase(viral) N terminal domain, 232R; dual specificity protein phosphatase, 123R; fasciclin, 96L; lysosome-associated membrane glycoprotein, 061R; nucleotide triphosphate (NTP), 22L; protein disulfide isomerase, 453L; ranavirus enveloped homolog, 118L; ribonuclease III, 142R; serine-threonine kinase, 209R, 380R, 439R and tyrosine protein kinase, 179R.

2.3 Apoptosis

The term apoptosis was first used by Kerr and his colleagues in 1972, to identify a different form of cell death. Apoptosis is a cascade of biochemical processes that leads to several morphological changes in the cell such as chromatin condensation, nuclear fragmentation and cell blebbing, the formation of apoptotic bodies, cytoplasmic shrinkage, detachment from neighbouring cells and finally phagocytosis of apoptotic bodies. Apoptosis is triggered by an extrinsic or intrinsic pathway (Figure 2.6). The extrinsic pathway is started by the interaction of Tumor Necrosis Factor (TNF) or Fas-ligand receptors with signals from outside of the cell. The intrinsic pathway relies on signals from cell mitochondria (45).

In both pathways, caspases are the main proteases responsible for apoptosis. Caspases are cysteine proteases that are found in their inactive form (zymogens, pro-caspases), and there are two kinds: initiator and executioner. Initiator caspases start a chain reaction that causes activation of executive caspases that are degraded over 600 cellular components. Caspases are activated by dimerization and cleavage.

Dimerization is facilitated by binding to an adaptor protein in the caspase structural domain with protein-protein interaction motifs, referred to as death fold. Death fold in the initiator intrinsic caspases includes one death fold called caspase recruitment domain (CARD) and initiator extrinsic caspases include two death folds known as death effector domains (DED). These domains are essential for the activation of caspase because for the apoptotic signalization an adaptor protein has to bind to initiator caspase, which can be done by CARD-CARD interactions or DED-DED interactions (46).

In the extrinsic pathway, cell surface death receptors (TNF and Fas ligand) constitute a death-inducing signal complex (DISC) that directly activates a caspase. The complex can be formed by DED domains. This activation results in the activation of executive caspase which causes the apoptosis. Apoptosis in insects is well understood in the Drosophila melanogaster model, where one mechanism comprises the interaction of Eiger (invertebrate TNF ligand) with a membrane receptor. This interaction leads to the activation of c-Jun N-terminal kinase (JNK), which results in the activation of initiator caspase Dronc that induces a cascade event of caspases to cause cell apoptosis (46).

In the intrinsic pathway, mitochondrial stress triggers permeabilization of the mitochondrial membrane, resulting in the release of mitochondrial intermembrane space proteins (Smac/Diablo, cytochrome c) into the cytosol. Cytochrome C binds to Apaf-1 (Apoptotic protease activating factor 1) through CARD-CARD interaction. This binding forms a heptamer is known as an apoptosome, which causes activation of initiator caspase. This is turn causes caspase cascade events and results in apoptosis (46).

Apoptosis is also known as a homeostasis event. For example, 20 to 30 billion cells die per day in human children aged 8 to 14. Next to apoptosis activators, there are various anti-apoptotic agents: In the intrinsic pathway, Bcl-2 is a kind of principal inhibitory agent which blocks apoptosis by binding to Apaf-1, resulting in preventing activation of caspase. Furthermore, cellular inhibitors of apoptosis (c*iap*) are

antiapoptotic entities which potentially play a role in inhibiting apoptosis in either the extrinsic or intrinsic pathway (46).

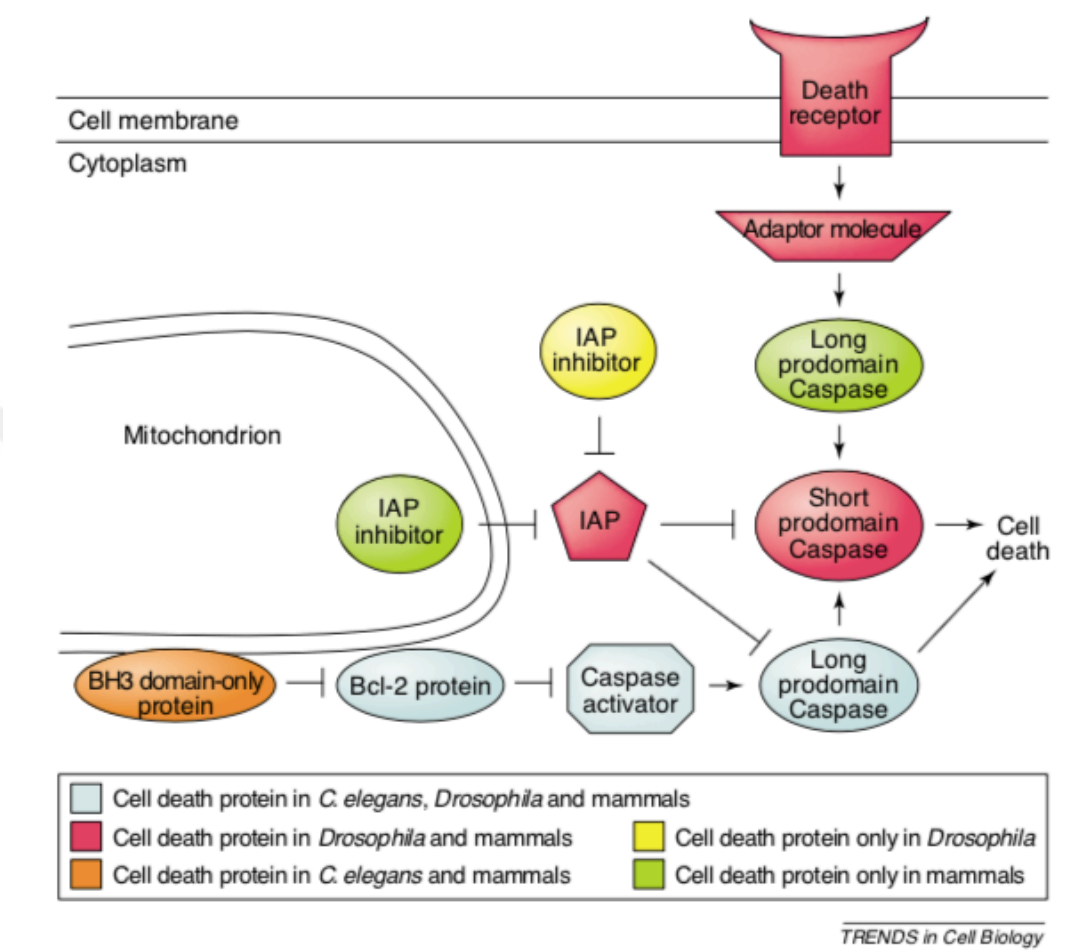

Figure 2.6 Brief overview of apoptosis.
Ref (47): Abraham MC, Shaham S. Death without caspases, caspases without death. Trends Cell Biol. 2004;14(4):184–93.

In addition, there is another way of inhibition and activation of apoptosis. In the chapters above, caspase-dependent apoptosis is mentioned, but recent work on mice and *Caenorhabditis elegans* showed caspase-independent apoptosis, and studies have also shown that caspase activation does not always result in apoptosis (47). Caspase-independent apoptosis pathways include various proteins such as AIF, Bak and Bax in mammals and CED-4 in *C. elegans*. Finally, many cells undergo apoptosis following viral infections. This apoptosis can be either a defence mechanism of the cell caused by the cell itself, or it can be an advantage for the virus, helping it to produce progeny.

2.3.1 Viral Apoptosis

Not surprisingly, viruses have evolved with their host mechanism. This mechanism can be a survival advantage to either host cell or virus. Advantage mechanisms involved are: (i) host cell induced apoptosis to prevent production and release of viral progeny; (ii) A viruses can prevent the host cell from inducing apoptosis early on in the infection to maximize production of their progeny or to assist the progress of viral persistence; (iii) A virus can induce apoptosis later on in the infection in order to spread their progeny to other uninfected cells (48). Viral apoptotic inhibition is conducted by an *iap* (see 1.3). The *iap* gene comprises RING finger and B1R domain, while *iap* genes that do not contain these domains, can be suggested to not be directly inhibiting apoptosis (20). Three gene of IIV-6 (157L, 193R, and 332L) are homolog with the *iap* gene of a baculovirus. Of these genes, the apoptotic function of 157L and 332L *iap* are not evaluated, but these genes contain only the RING domain, lacking the BIR domains. 193R contains both domains and is also confirmed as a functional *iap* gene (7).

In addition, IIV-6 also induces apoptosis. A study showed that a virion protein extracted from IIV-6, induces apoptosis in spruce budworm and boll weevil cell lines. But kinase activity was also detected in the virion protein extract (49). In the another study, Chitnis et al showed that IIV-6's 389L gene protein induces apoptosis. Iridoptin protein 389L was isolated from the *Pichia pastoris* system, and their apoptosis interaction with the host cell was determined by the TUNEL blebbing assay method. Furthermore, they defined the actual site of 389L which is a 35 k-DA cleavage product (10). However, the apoptotic function of 389L was determined only at the protein level, the apoptotic function of 389L as a part of IIV-6 has not been evaluated. Also, the effect of 389L on viral infectivity was not evaluated. ORF 389L was knock-outed and over-expressed in a recombinant virus, and this recombinant virus was then studied to gain an understanding of the apoptotic role of IIV-6 389L gene at the genomic level. In addition, this is the first time the effect of 389L on viral infectivity was evaluated. Furthermore, this thesis may serve as a guideline for understanding the

apoptotic interaction of double-strand DNA viruses with their host, and for determining the effect of kinase genes on viral replication.

3. MATERIALS AND -METHODS

3.1 Virus, Cell and Model Insect

IIV-6 was supplied by Dr C. Joel Funk (USDA-ARS Western Cotton Research Laboratory, USA). For virus rearing, *Galleria mellonella* was infected with IIV-6. The cells used in this thesis were *Spodoptera frugiperda* ovary cells (SF9). Express Five SFM medium supplied with 10% FBS was used for both cell growth and experiments.

3.2 Virus Rearing and Isolation

IIV-6 was propagated in the larvae of the greater wax moth, *Galleria mellonella,* by an injector. A frozen larva of *G.mellonella* that had previously been infected with IIV-6 was homogenized in 1 ml ddH_2O. The homogenate was centrifuged for 10 minutes at 490g, 960g, and 1.250g respectively to remove tissue particles. Then the virus was centrifuged at 15.300 g. The precipitate was dissolved in 500 µl ddH_2O with 30% sucrose solution. This mixture was centrifuged at 15.300 g for 30 minutes. The precipitate was cleaned once with ddH_2O and dissolved in 1 ml ddH2O. The purified virus was filtrated into sterile tubes and kept at +4 °C. For the viral propagation in the cell culture, SF9 cells were infected at a confluence of 80-90% with 5 µg IIV-6 per ml culture, being shaken at a speed of 5 rpm for 2 hours.

3.3 Bioinformatic analysis of 389L gene

Protein comparisons in the GenBank were performed with the NCBI/BLAST programs. Serine-threonine gene of Vaccinia Virus (NCBI:txid696871), Lumpy skin disease virus (NCBI:txid376849), Yaba monkey tumor virus (NCBI:txid38804), Myxoma virus (NCBI:txid31530), *Amsacta moorei* entomopoxvirus (NCBI:txid28321) were selected for alignment with IIV-6 389L gene. Sequence alignment was completed with the ClustalW program (EMBL, European

Bioinformatics Institute, http://www.ebi.ac.uk) and edited with the BioEdit software tool (version 7.2) (50).

3.4 Generation of the Recombinant Virus

The IIV-6 ORF 389L of the w/t IIV-6 genome was replaced with an enhanced green fluorescent protein gene (eGFP) to knock-out 389L. The Major Capsid Protein (*mcp*) gene promoter of IIV-6 was used as a promoter for eGFP expression. As promotor of *mcp* gene is a strong promoter of IIV-6, it was likewise used to over-express 389L. A destination plasmid was generated separately for all of the sequences. Sequences were digested with different restriction enzymes from destination plasmid and ligated to a main recombinant plasmid for knock-out and over-express, separately. A series of sequences from the top and bottom part of the ORF 389L were identified as upstream and downstream. For the homolog recombination of the targeted regions, knock-out recombination (k/r) plasmid was generated to be upstream, *mcp*-eGFP, downstream, respectively, and over-express recombination (o/r) plasmid was generated to be upstream, *mcp*-eGFP, *mcp*-389L, downstream, respectively. Similarly, the 299 bp *mcp* promoter that includes the 18 bp *mcp* gene with start codon, the 717 bp eGFP without a start codon, the 650 bp upstream and the 664 bp downstream sequence of 389L were cloned to k/r plasmid. In addition to the k/r plasmid, ORF 389L of w/t IIV-6 with *mcp* promoter similar to the other *mcp* was also cloned to o/r plasmid. To get homolog recombination to occur, SF9 cells were first infected with w/t IIV-6; then transfected with recombination (k/r and o/r) plasmids. Cells that were emitting a fluorescent signal were selected as recombinant IIV-6.

3.4.1 Polymerase Chain Reaction (PCR)

For the homolog recombination of the targeted regions, a series of sequences from the top and bottom part of the ORF 389L were identified as upstream and downstream and selected regions were cloned as starting sequences in the recombination plasmids.

To obtain these regions and also other regions that are IIV-6 *mcp* promoter, eGFP, and 389L, different primers (P) with restriction digestion sequences were designed for a Polymerase Chain Reaction (PCR) (Table 3.1). The 389L, the determined upstream and downstream of 389L and an *mcp* promoter that includes the 18 bp *mcp* gene were amplified from CIV DNA, and eGFP was amplified from pIRES2-eGFP plasmid that was kindly supplied by Dr Emre Deniz.

Table 3.1 Primer sequences used in generating a recombinant virus experiment (The enzyme sequences are underlined)

No:	Primer Name	Primer Sequence (5' - 3')
P1	CIV 389L Ups Fw	CGAGCTCCAATCTCTTTCATTTTGTTTAATT
P2	CIV 389L Ups Rv	TTGCGGCCGCTTTGTGTCATTAAAAATGTTTATA
P3	CIV 389L Ds Fw	CCGCTCGAGCATATT TAA CTAATT TTTATTTTA
P4	CIV 389L Ds Rv	GGGGTACCGGTGAAAAATTAGATATTGCAGTT
P5	CIV 389L Fw	CAAAGATGTCTATTTCTTCGTCAGATCTTAAAGACGAATTTATT
P6	CIV 389L Rv	CCGCTCGAGTTAGTTAAAAATGTTATGTAATAG
P7	*mcp*389L Fw	CCCAAGCTTCAATACATAACAATCTTTCATTAT
P8	*mcp*389l Rv	AATAAATTCGTCTTTAAGATCTGACGAAGAAATAGACATCTTTG
P9	eGFP Fw	CAAAGATGTCTATTTCTTCGTCAGTGAGCAAGGGCGAGGAGC
P10	eGFP Rv	CCCAAGCTTTTACTTGTACAGCTCGTCC
P11	*mcp*eGFP Fw	TTGCGGCCGCCAATACATAACAATCTTTCATTAT
P12	*mcp*eGFP Rv	GCTCCTCGCCCTTGC TCACTGACGAAGAAATAGACATCT TTG

Six different DNA regions were amplified by PCR using primer sets. 650 bp upstream of IIV-6 389L using the P1/P2 primer set, 664 bp downstream of IIV-6 389L using the P3/P4 primer set, 1532 bp IIV-6 389L using P5/P6, 299 bp *mcp* promoter including the 18 bp *mcp* gene using P7/P8, 717 bp eGFP from pIRES2-eGFP plasmid using P9/P10 and the *mcp* promoter that includes the 18 bp *mcp* gene using P11/P12. w/t IIV-6 DNA was used as template DNA for *mcp*, Downstream of 389L, Upstream of 389L and 389L amplification PCR. After PCR, 389L and the *mcp* promoter; eGFP and the *mcp* promoter were fused by fusion PCR. The *mcp* promoter for 389L and the *mcp* promoter for eGFP are different from each other, the difference originating from the presence of restriction enzymes in the primer sequences. Phusion Green High-Fidelity DNA Polymerase (Thermo Scientific, Catalog No: F534S) featuring an error rate 50-fold lower than that of Taq polymerase, with 3'-5' exonuclease activity was used as

DNA polymerase for PCR reactions. According to the manufacturer's instruction, the PCR mixture (Table 3.2) and PCR conditions (Table 3.3) were used. Extension time depended on the length of the fragments.

Table 3.2 PCR mixture and final concentration

PCR mixture		**Final Concentration**
DNA	10 ng	
Forward Primer (10 µM)	1.5 µl	0.3 µM
Reverse Primer (10 µM)	1.5 µl	0.3 µM
dNTP (10 mM)	1.5 µl	200 µM
5X Phusion HF Buffer	10 µl	1X
dH_2O	Added to 50 µl	
Phusion Enzyme (2U/µl)	0.5 µl	0.02 U/µl

Table 3.3 PCR conditions

Cycle Step	**Temperature**	**Time**	**Cycles**
Initial Denaturation	98 °C	30 seconds	1 cycle
Denaturation	98 °C	10 seconds	
Annealing	55 °C	30 seconds	35 cycle
Extension	72 °C	30 seconds/kb	
Final Extension	72 °C	10 minutes	1 cycle

3.4.1.1 Purification of the PCR Product

The PCR product for all DNA regions was purified using the Zymoclean™ Gel DNA Recovery Kit (Cat.No: D4001). The DNA band of interest was excised from 1% agarose gel using a razor blade and dissolved in Agarose Dissolving Buffer (ADB), then the mixture was incubated at 55 °C for 15 minutes. The melted agarose solution was loaded into the kit column using a centrifuge. After binding to the column, the column was washed with kit washing buffer. After washing, the pure DNA was eluted in dH_2O.

3.4.1.2 Fusion PCR

The P6, P7 primer set was used to fuse the *mcp* promoter to 389L, and the P10, P11 primer set was used to fuse the *mcp* promoter to eGFP (Figure 3.1).

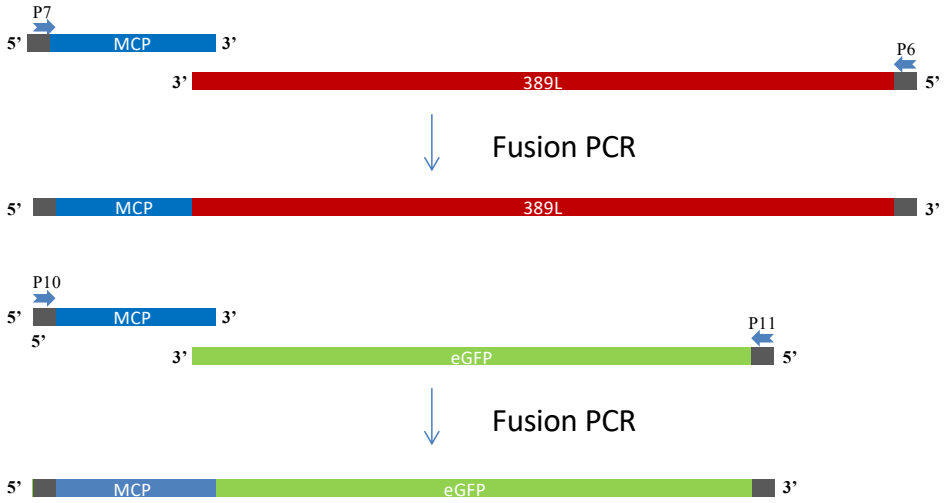

Figure 3.1 fusion PCR of the *mcp* promoter to 389L and eGFP. The image represent single strand of DNA.

The *mcp* promoter, 389L and the eGFP PCR product were purified from agarose gel before the fusion PCR. After that, the PCR product of *mcp* promoter was fused with eGFP and 389L separately. In the fusion PCR, desired sequences to be fused were used as a template in the PCR mixture and PCR conditions were applied similar to the PCR conditions in Table 3.3 (Table 3.4).

Table 3.4 Fusion PCR mixture and final concentration

PCR mixture		Final Concentration
DNA 1	10 ng	
DNA 2	10 ng	
Forward Primer (10 µM)	1.5 µl	0.3 µM
Reverse Primer (10 µM)	1.5 µl	0.3 µM
dNTP (10 mM)	1.5 µl	200 µM
5X Phusion HF Buffer	10 µl	1X
dH_2O	Added to 50 µl	
Phusion Enzyme (2U/µl)	0.5 µl	0.02 U/µl

3.4.2 Constructing Cloning Plasmid

Fused *mcp* and 389L, and fused *mcp* and eGFP, upstream of 389L and downstream of 389L were ligated to pJET 1.2/blunt plasmid (Thermo, Cat. No: K1231). After ligation, the ligation mixture was transformed into a competent *Escherichia coli* DH5α strain according to heat-shock protocol. After the transformation, the bacterial mixture was plated on LB agar containing 100 µg/ml ampicillin for 16 hours. Growth colonies were screened by colony PCR using the interested sequence primers (Table 2.1). Colony PCR products were analyzed by electrophoresis through a 1% agarose gel. The cells that contained the plasmid which was observed in the agarose gel, were incubated at 37 ºC in liquid LB medium with shaking at 180 rpm. The plasmid was isolated using Zyppy™ Plasmid Miniprep Kit (Zymo, Cat. No: D4036). Isolated plasmids were digested with BglII restriction enzyme (Thermo Scientific, ER0081). The digested plasmid was confirmed by 1% agarose gel electrophoresis. For the additional confirmation, the confirmed plasmid was sequenced by Macrogene Europe Ez-seq service.

3.4.2.1 Ligation

As can be seen in the ligation reaction mixture below (Table 3.5), inserts were ligated to pJET 1.2/blunt plasmid (Thermo, Cat. No: K1231). The amount of DNA fragmented with pJET 1.2 was calculated with a ligation calculator program (IN.SILICO Online Bioinformatics Resources) available online.

Table 3.5 Ligation Mixture

Component	Volume
2X Reaction Buffer	10 µl
Purified-PCR product	Depends on DNA amount
pJET 1.2/blunt plasmid (50 ng/µl)	1 µl
Water / nuclease free	Up to 20 µl
T4 DNA Ligase	1 µl

3.4.2.2 Transformation

An *Escherichia coli* DH5α strain was used to make a competent cell using an improved buffer (2M $CaCl_2$, 100% (v/v) glycerol). *E.coli* DH5α liquid LB Broth culture was incubated at 37°C while shaking at 180 rpm until the culture optical density (OD) reached a range of 0.35-0.45. Bacterial OD was measured by a spectrophotometer at 600 nm. When the culture reached desired OD, it was pelleted with a centrifuge at 10.000 g for 10 minutes at +4°C. The pellet was solved with improved buffer and incubated at +4°C for 15 minutes. The solution was centrifuged at 1.000 g for 10 minutes at +4°C. After the centrifugation, the pellet was solved in improved buffer which includes 2M $CaCl_2$ and %100 Glycerol and stored in small aliquots at -80 °C. 10 µl ligation mixture (Table 2.5) was mixed with 50 µl chemically competent *E.coli* DH5α brought from a -80°C freezer. The mixture was incubated at +4°C for 30 minutes and then incubated at 42°C for 2 minutes for heat-shock. Then, 1 ml LB broth (without antibiotic) was added to the transformation mixture and incubated at 37°C for 2 hours with shaking at 180 rpm. After 2 hours, the mixture was pelleted with a centrifuge at 6.000 RCF for 3 minutes. The LB broth was discarded, leaving 50 µl of

Broth at the end of the tube and this remaining mixture was spread with a bacterial L loop onto a bacterial plate (90X11 mm in dimension) that included ampicillin for selection. The plate was incubated at 37°C for 16 hours.

3.4.2.3 Colony PCR

Colonies were screened by colony PCR with corresponding primers in Table 2.1. Tag polymerase was used to catalyze PCR and colonies were selected with an autoclaved toothpick as the DNA template. PCR mixture and PCR conditions are given below (Table 3.6).

Table 3.6 Colony PCR Mixture and PCR conditions

PCR mixture		**PCR conditions**		
$MgCl_2$	1,2 µl	Initial Denaturation	98°C	30"
Forward Primer (10 µM)	0.4 µl	Denaturation	98°C	10"
Reverse Primer (10 µM)	0.4 µl	Annealing	55	30"
dNTP (10 mM)	0.4 µl	Extension	72°C	2'
10X Phusion HF Buffer	2 µl	Final Extension	72°C	10'
dH_2O	Added to 20 µl			
Tag Polymerase (2U/µl)	0.5 µl			

20 Cycle

3.4.2.4 Plasmid Isolation

E.coli DH5α colonies that probably include targeted DNA fragments were grown at 37°C overnight. Targeted plasmids were isolated from the overnight culture using Zyppy™ Plasmid Miniprep Kit (Zymo, Cat. No: D4036). The protocol was conducted according to the manufacturer's protocol and DNA was eluted with dH2O. Plasmids were digested with a BglII restriction enzyme (Thermo Scientific, ER0081) that has two digestion sites in pJET 1.2 to determine the presence or absence of insert DNA in the plasmid construct. After preparing the digestion mixture (Table 3.7), it was

incubated at 37°C for 4 hours. At the end of the digestion process, the mixture was screened using 1% agarose gel electrophoresis. The confirmed positive plasmid was sequenced by Macrogene Europe Ez-seq service. pJET 1.2 forward and reverse primers were used for sequencing and the sequence result was analyzed using the Basic Local Alignment Search Tool (BLAST / NCBI).

Table 3.7 Digestion Reaction Mixture

Component	**Volume**
10X Fast Digest Buffer	10 µl
Purified-PCR product	1000 ng (final concentration)
BglII fast digest enzyme	1 µl
Water / nuclease free	Up to 40 µl

3.4.3 Constructing Recombination Plasmid (pBlueScript (-))

pJET 1.2 plasmids that included the targeted insert sequences were digested with a restriction enzyme with a digestion site in the primer regions (Table 3.8). At the same time, to achieve sticky ends at the end of the sequences, recombination plasmid pBlueScript (-) was digested with the enzyme that was used in the pJET 1.2 plasmid digestion. The sticky ends were used to clone the insert sequence to the recombination plasmid. The entire digestion reaction was conducted using the same reaction mixture, described in part 2.5.2.4 (Table 3.7). The entire digestion reaction was performed at 37 °C for 4 hours.

Table 3.8 Restriction Enzymes That Cut the Insert Regions

Insert	Restriction Enzyme	Cutting End
Upstream of 389L	Sac1	5'
	Not1	3'
mcp-eGFP	Not1	5'
	Hind3	3'
mcp-389L	Hind3	5'
	Xho1	3'
Downstream of 389L	Xho1	5'
	Kpn1	3'

The upstream sequence of 389L, the *mcp*-eGFP fused sequence, the *mcp*-389L fused sequence, and the downstream sequence of 389L were cloned using restriction enzyme in the recombination plasmid. In addition to the knocked-out plasmid inserts, mcp-389L insert was cloned in the over-express recombination plasmid (Figure 3.2)(Figure 3.3).

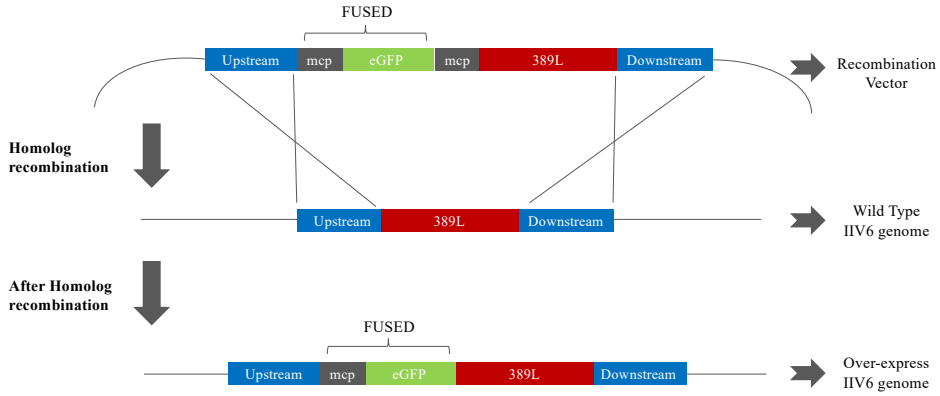

Figure 3.2 homolog recombination using o/r plasmid

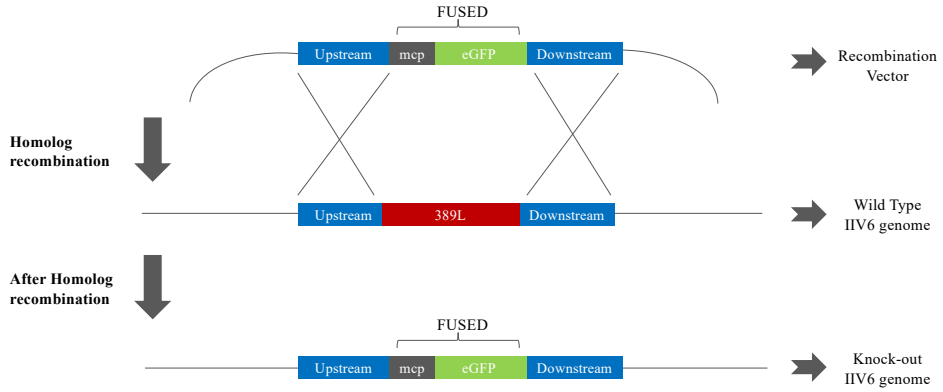

Figure 3.3 homolog recombination using k/r plasmid

3.5 Transfection of Recombination Plasmid

Before transfection, IIV-6 infection was conducted with the method covered in part 2.2. After infection, solution A, including 6 µg plasmid and a cell medium (completed to 100 µl) and solution B (12 µl PEI transfection reagent and 88 µl cell medium) were prepared. These solutions were incubated at room temperature for 20 minutes. After incubation, the solutions were mixed. The mixture was incubated at room temperature for another 45 minutes. In this time, the cell that was going to be used for transfection was cleaned with medium (without FBS). After 45 minutes, (another) 800 µl cell medium (with FBS) was added to the mixture. Then, the total mixture was added to the cleaned cell, and the cell was incubated at 28 °C for five hours. After incubation, the transfection mixture was removed, and the cell medium was added.

3.6 Plaque Assay

After the IIV-6 infection was conducted as described in part 2.2. 2.5% low-melt agarose was prepared and sterilized with an autoclave (121 °C at 15 min). Cell medium with FBS was mixed with 2.5% agarose at a 1/1 ratio and the mixture was kept at 42 °C. The infection solution (IIV-6) was removed from the cell surface. Agarose-medium mixture was added to the infected cell. After the mixture was solidified at

room temperature for about 15 minutes, the mixture was incubated in an area containing high humidity at 28 °C. The plaque was then visualized using a Zeiss AX10 microscope (Carl Zeiss, USA). Approximately 72 hours later, the plaque including the GFP signal (recombinant virus) was selected, and used for a second infection, to purify the recombinant virus. This plaque experiment was conducted 8 times.

3.7 Quantification of Purified Recombinant IIV-6 and Wild type IIV-6

Purified recombinant viruses were propagated in a 75 cm2 cell flask to obtain stock. Infected SF9 cells were incubated at 28 °C until a signal of infection was obtained. At the end of the infection, the infected cell suspension was centrifuged at 1000 g for 5 minutes. The supernatant was centrifugated again at 20.000 g for 30 minutes to achieve viral stock. The titer of viruses was determined by the Tissue Culture Infectious Dose; TCID50 method. To determine titration, viruses were diluted in 10 fold series, 50 ml of the diluted virus was used to infect SF9 cells, and each dilution in the 96 well plates was infected. Viruses were allowed to attach to and infect cells by incubation for 2 h at 28 °C. Each dilution was repeated 6 times, and the TCID50 assay of each virus was also repeated 3 times. After observing the virus symptoms, every well was evaluated for infection. Each concentration was determined by evaluating positive infected wells in the 96 wells (Figure 3.4). The TCID50 is the antilog of each diluted well at which 50% of the wells are positive for the virus. To calculate the TCID50, we used the Spearman–Karber method as described by Hierholzer and Killington (51).

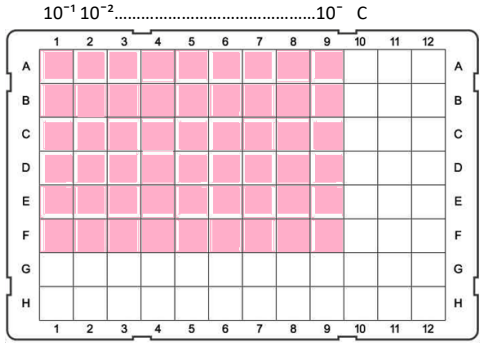

Figure 3.4 10-1 to 10-9 dilutions of w/t, k/o and o/e IIV-6 in the 96 wells where they are propagated.

3.8 Comparison of One-Step Growth Curves of Recombinant Viruses and Wild Type Virus

To compare the infectious roles of the viruses, one-step growth curve of the virus was conducted. To do this, 90% confluent SF9 cells were infected with a different type of IIV-6 (MOI=1, selected as 5.10^6 TCID50 per ml). After the initial infection, the infected cells were harvested at 0, 6, 12, 18, 24, 36, 48 and 72 hours. The harvested cells were centrifugated and collected for the quantification of the virus as mentioned in part 3.7. The experiment was repeated three times. Non-infected SF9 cells were defined as the control group. After the quantification of the virus, the growth curves were determined.

4. RESULTS

4.1 Bioinformatic analysis of 389L gene

Multiple alignments of IIV-6 389L gene protein with protein sequences of viral serine-threonine gene homologues were aligned using the ClustalW program and edited with the BioEdit program.

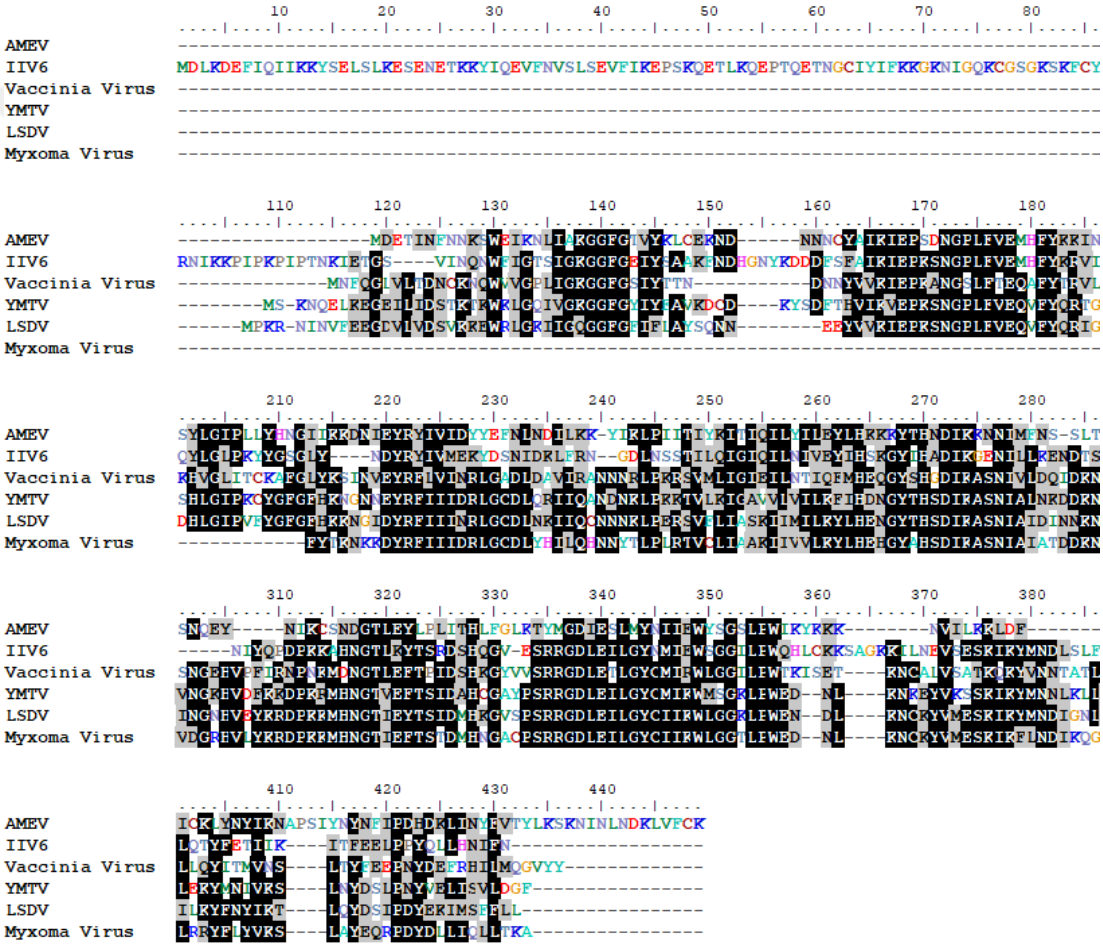

Figure 4.1 Multiple alignments of IIV-6 389L gene protein with protein sequences of viral serine threonine gene homologues. Light grey and black column indicate amino acids with ≥ 80 similarities an ≥ 95 similarities, respectively. AMEV: *Amsacta moorei* entomopoxvirus (NCBI:txid28321), IIV-6: Invertebrate Iridescent Virus 6, Vaccinia Virus (NCBI:txid696871), YMTV: Yaba monkey tumor virus (NCBI:txid38804), LSDV: Lumpy skin disease virus (NCBI:txid376849), Myxoma virus (NCBI:txid31530).

4.2 Generation of the Recombinant Virus

4.2.1 Polymerase Chain Reaction (PCR)

To generate the transfer plasmid, upstream (Figure 4.1) and downstream (Figure 4.1) of IIV-6 389L (Figure 4.2), all of the 389L gene (Figure 4.3), and *mcp* ORF (Figure 4.4) was amplified by PCR. The sequence of PCR results was shown by gel electrophoresis method. The gel electrophoresis image is given below.

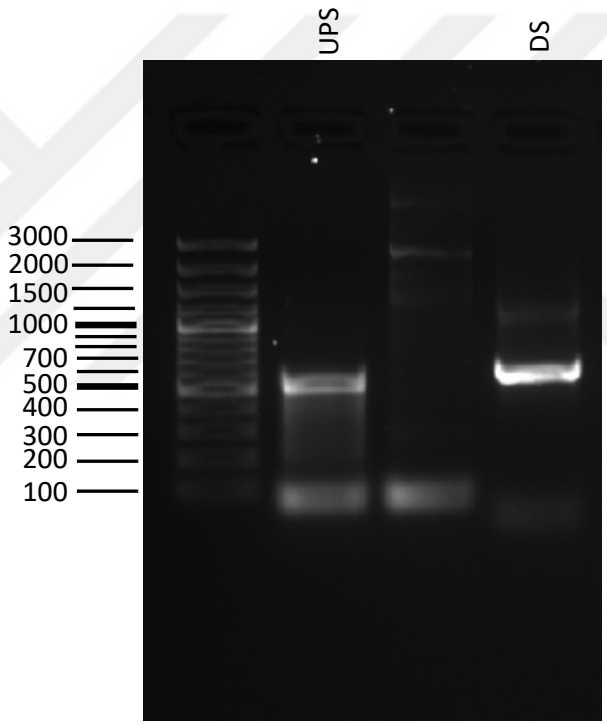

Figure 4.2 1.well; Marker, 2.well; upstream of 389L sequence, 3.well; Irrelevant, 4. Well; downstream of 389L. Marker order: 100 bp, 200 bp, 300 bp, 400 bp, 500 bp, 600 bp, 700 bp, 800 bp, 900 bp, 1 kb, 1.1 kb, 1.5 kb, 2 kb, 3 kb. Bold sequences are shown as more visible bands in the gel.

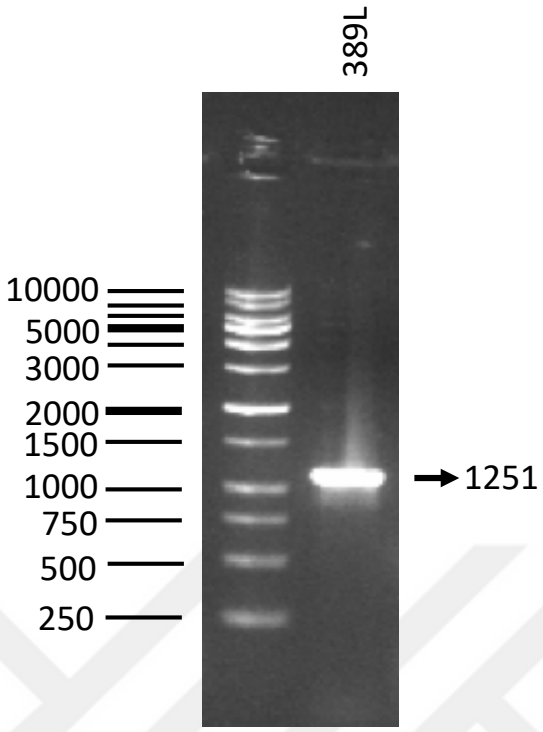

Figure 4.3 1.well; Marker; 2.well; 389L sequence. Marker order: 250 bp, 500 bp, 750 bp, 1 kb, 1,5 kb, 2 kb, 3 kb, 4 kb, 5 kb, 6 kb, 8 kb, 10 kb. Bold sequences are shown as more visible bands in the gel.

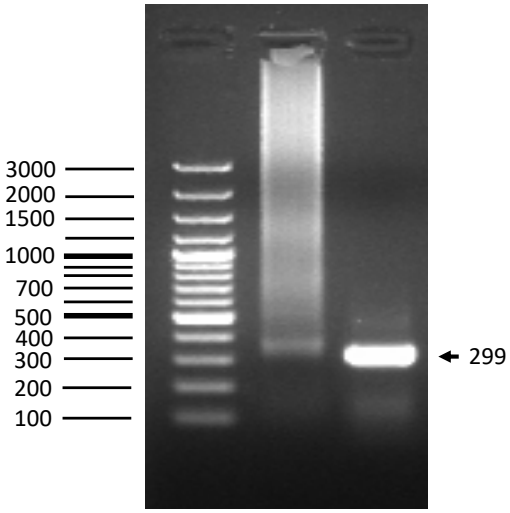

Figure 4.4 1.well; Major Capsid Protein gene promoter of IIV-6 (mcp), 2.well; Irrelevant, 3.well; Marker. Marker order: 100 bp, 200 bp, 300 bp, 400 bp, 500 bp, 600 bp, 700 bp, 800 bp, 900 bp, 1 kb, 1.1 kb, 1.5 kb, 2 kb, 3 kb. Bold sequences are shown as more visible bands in the gel.

4.2.2 Formation of the Destination Plasmid

Before the generation of the recombinant virus plasmid that was used for homolog recombination, upstream (Figure 4.5) and downstream (Figure 4.6) of IIV-6 389L, ORF 389L (with *mcp* promoter) (Figure 4.7), *mcp* promoter, and eGFP (with *mcp* promoter) (Figure 4.8) regions were cloned to pJET 1.2 plasmid in order to obtain a large amount of DNA, and for accurate restriction digestion. Confirmation of pJET 1.2 cloning is given below.

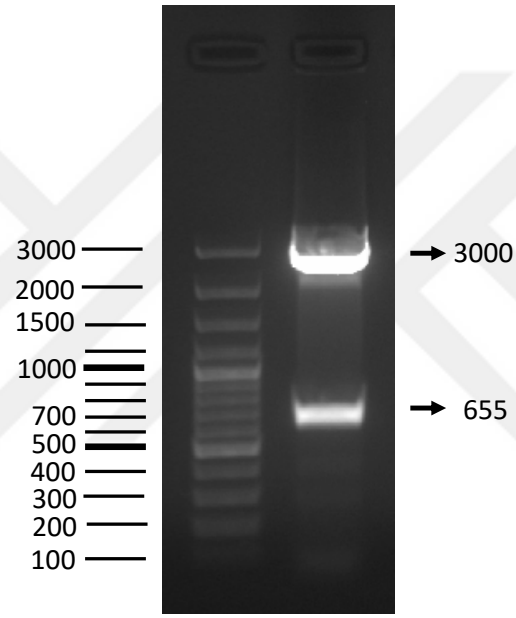

Figure 4.5 1.well; Marker; 2.well; upstream of 389L sequence in pJET 1.2 plasmid digested with Not1 and Sac1 enzyme (UPSpJET). Marker order: 100 bp, 200 bp, 300 bp, 400 bp, 500 bp, 600 bp, 700 bp, 800 bp, 900 bp, 1 kb, 1.1 kb, 1.5 kb, 2 kb, 3 kb. Bold sequences are shown as more visible bands in the gel.

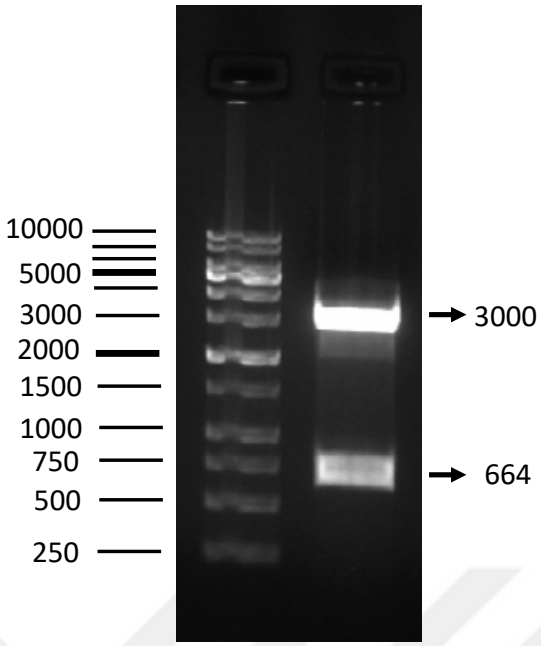

Figure 4.6 1.well; 1 Kb Marker, 2. Well; Downstream of 389L sequence in pJET 1.2 plasmid digested with Xho1 and Kpn1 enzyme (DSpJET). Marker order: 250 bp, 500 bp, 750 bp, 1 kb, 1,5 kb, 2 kb, 3 kb, 4 kb, 5 kb, 6 kb, 8 kb, 10 kb. Bold sequences are shown as more visible bands in the gel.

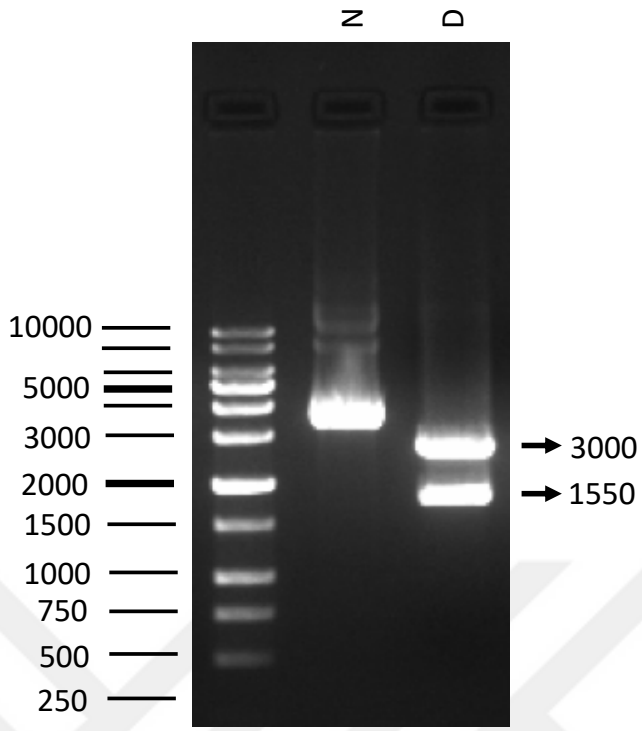

Figure 4.7 1.well; 1 Kb Marker, 2. Well; (N) Non-digested 389L (with mcp) in pJET 1.2 plasmid digested with Xho1 and Kpn1 enzyme (DSpJET), 3. Well; (D) Digested 389L (with mcp) in pJET 1.2 plasmid (digested with Xho1 and Kpn1 enzyme). Marker order: 250 bp, 500 bp, 750 bp, 1 kb, 1,5 kb, 2 kb, 3 kb, 4 kb, 5 kb, 6 kb, 8 kb, 10 kb. Bold sequences are shown as more visible bands in the gel.

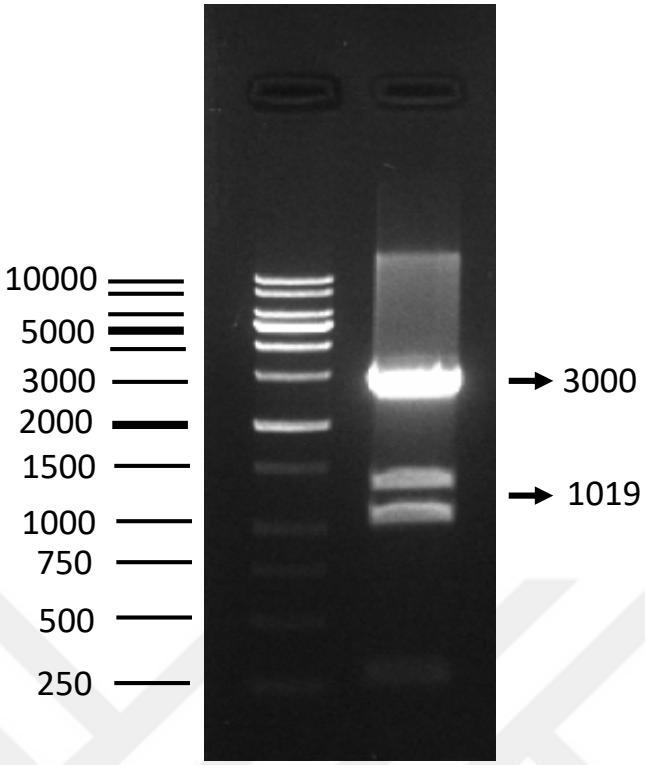

Figure 4.8 1.well; 1 kb Marker; 2.well; eGFP (with mcp promoter) in pJET 1.2 plasmid digested with Hind3 and Not1. Marker order: 250 bp, 500 bp, 750 bp, 1 kb, 1,5 kb, 2 kb, 3 kb, 4 kb, 5 kb, 6 kb, 8 kb, 10 kb. Bold sequences are shown as more visible bands in the gel.

4.2.3 Generation of Recombination Plasmid

The Recombination plasmid was generated by restriction enzyme digestion and ligation. The upstream region of 389L base pair is 650, downstream of 389L is 664, 389L (with *mcp* promoter) is 1535, and eGFP (with *mcp* promoter) is 1016. The expected plasmid base pair is 5330 for knocked out plasmid and 6865 for over-expressed plasmid. Knocked out plasmid comprises the upstream and downstream region of IIV-6 389L and eGFP (with *mcp* promoter), but over-expressed plasmid also contains 389L (with *mcp* promoter). To confirm cloning of desired regions, over-expressed plasmid and knock-outed plasmid was digested by an EcoR1 enzyme (Figure 4.9).

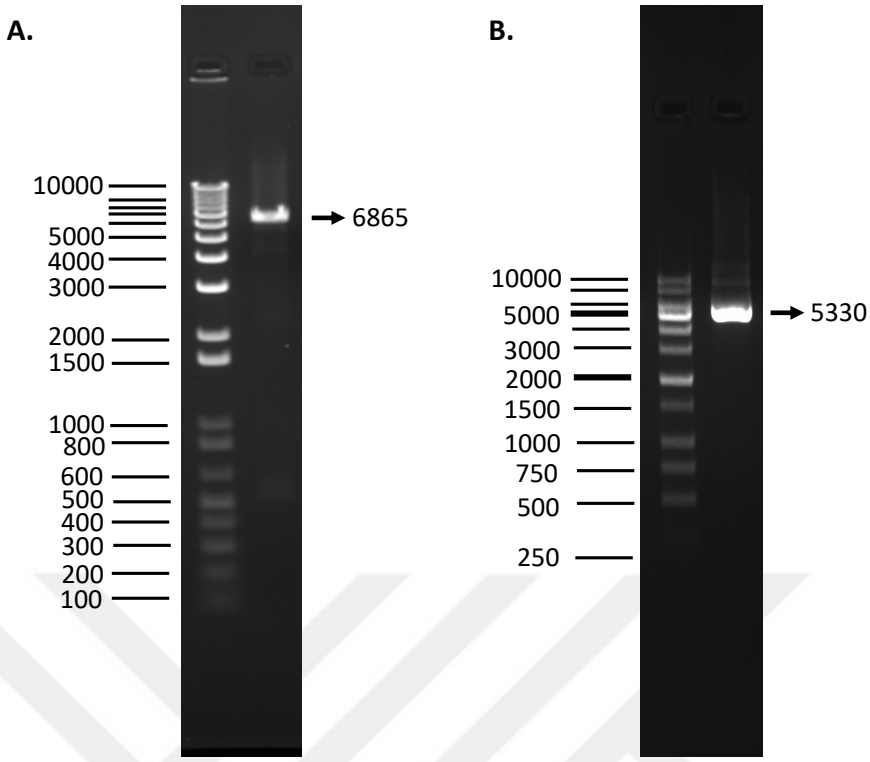

Figure 4.9 A: 1.well, Marker, 2. Well Over-expressed plasmid (6865 bp). Marker order:100,200,300,400,500,600,800,1000,1500,2000,3000,4000,5000,6000,7000,8000,9000, 10000 bp. B: 1. Well; Marker, 2.well; Knock-outed plasmid (5330 bp). Marker order: 250 bp, 500 bp, 750 bp, 1 kb, 1,5 kb, 2 kb, 3 kb, 4 kb, 5 kb, 6 kb, 8 kb, 10 kb. Bold sequences are shown as more visible bands in the gel.

4.3 Transfection of Recombination Plasmids

6 ug knocked out and over-expressed plasmid was transfected with PEI transfection reagent into the IIV-6 infected SF9 cell line. Transfections were then visualized using a Zeiss AX10 microscope (Carl Zeiss, USA).

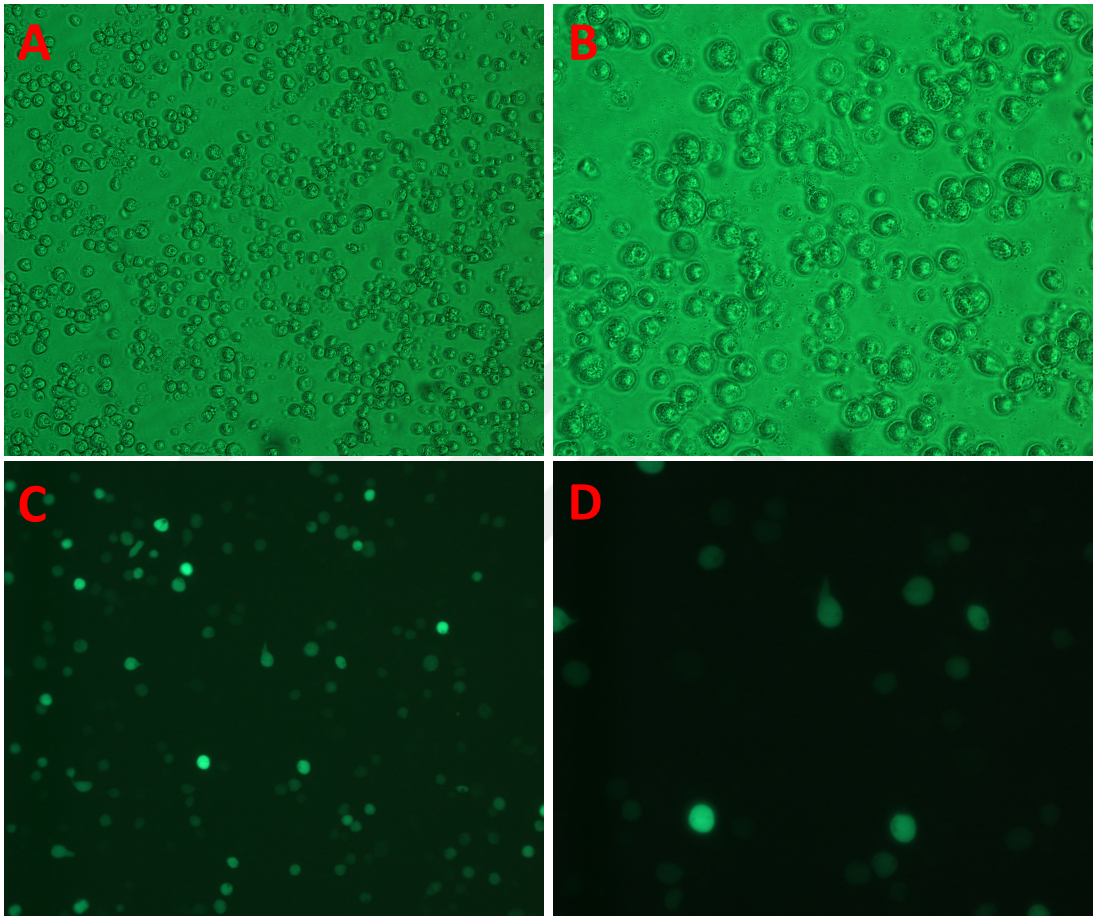

Figure 4.10 K/r plasmid was transfected with PEI. (A) Transmitted Light, Magnification X10; (B) Transmitted Light, Magnification X20; (C) Reflected Light, Magnification X10; (D) Reflected Light, Magnification X20. The cells were then incubated at 28°C for 72 h and observed for eGFP signal using a Zeiss AX10 (Carl Zeiss, USA).

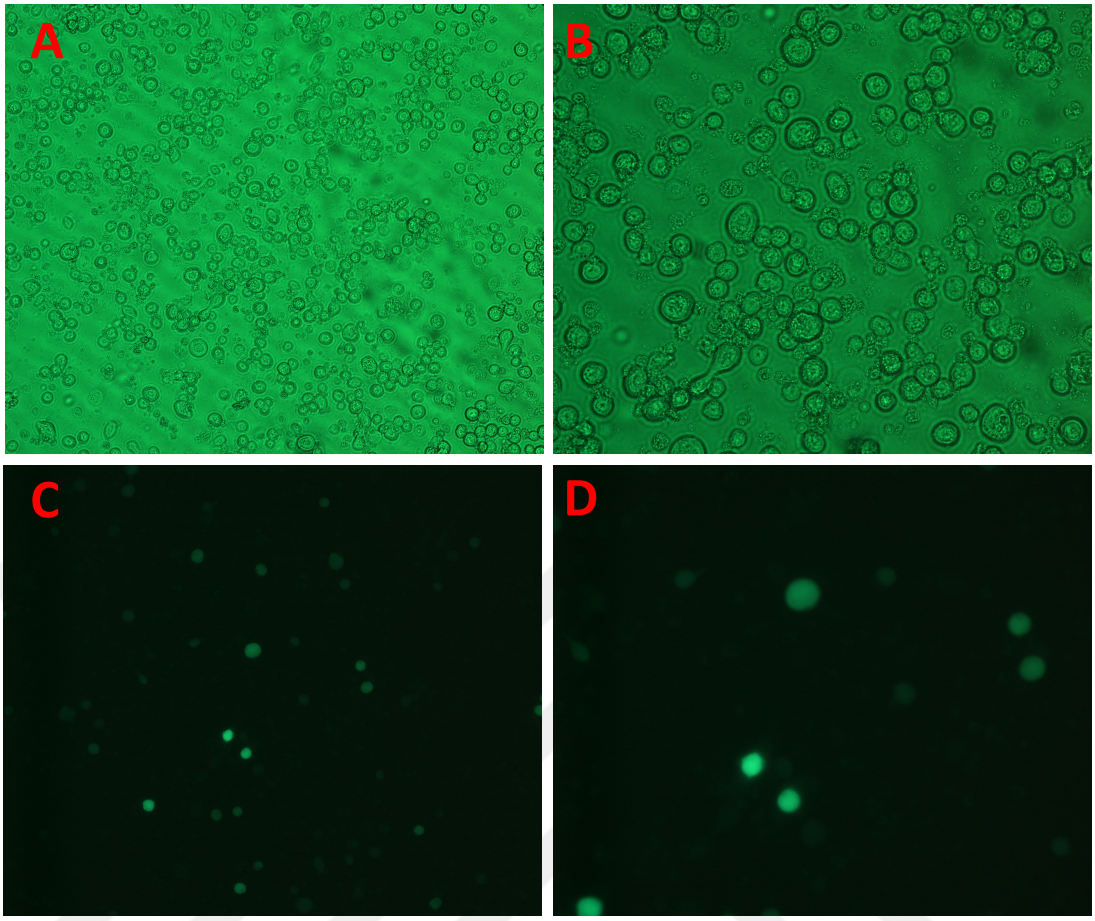

Figure 4.11 O/r plasmid was transfected with PEI. (A) Transmitted Light, Magnification X10; (B) Transmitted Light, Magnification X20; (C) Reflected Light, Magnification X10; (D) Reflected Light, Magnification X10. The cells were then incubated at 28°C for 72 h and observed for eGFP signal using a Zeiss AX10 (Carl Zeiss, USA).

4.4 Purification of Recombinant Virus with Plaque Assay

The recombinant viruses (knocked out and over-expressed) were purified by plaque assay method. Purity was assessed by the PCR method. 8 plaque assays were sufficient to reach the required purity of the recombinant viruses.

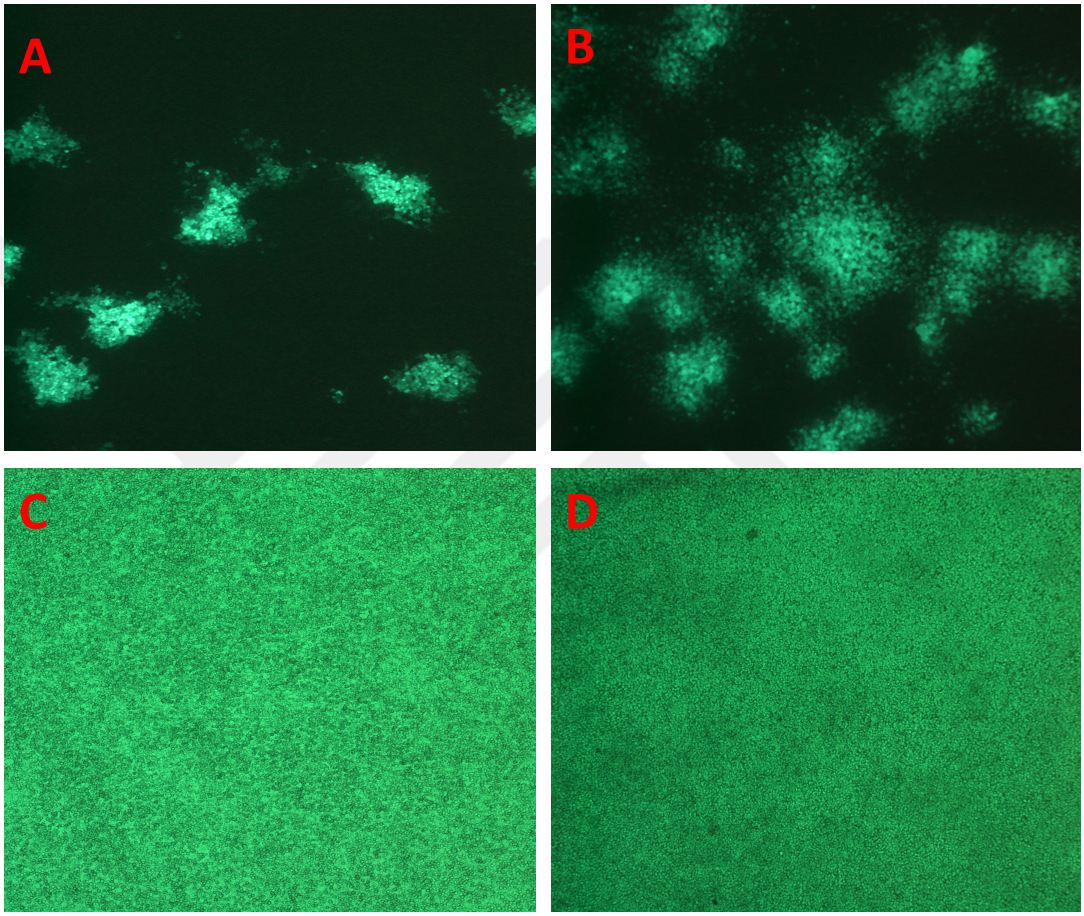

Figure 4.12 Plaque assay of o/e and k/o recombinant virus was obtained using a Zeiss AX10 microscope (Carl Zeiss, USA). Plaque can be clearly observed. (A) K/o Virus, Reflected Light, Magnification X4; (B) O/e Virus, Reflected Light, Magnification X4; (C) K/o Virus, Transmitted Light, Magnification X4; (D) O/e Virus, Transmitted Light, Magnification X4

4.5 Quantification of Purified Recombinant IIV-6 and Wild type IIV-6

The titer of stock recombinant viruses and the w/t virus was determined using the $TCID_{50}$ method (Table 4.1). To be able to do that, stock infection was propagated in the SF9 cell line. The Spearman–Karber method as described by Hierholzer and Killington (51) was used for the calculation of the $TCID_{50}$. For the one step assay, MOI=1 was determined as 5.10^6 TCID per ml.

Table 4.1 Virus Concentration

Virus Type	**Stock $TCID_{50}$ per ml**
Knock-Outed IIV-6	$7{,}317.10^7$
Over-Expressed IIV-6	$11{,}675.10^7$
Wild Type IIV-6	$3{,}245.10^7$

4.6 Comparing Growth Curves of IIV-6s

The SF9 cell was infected with three types of IIV-6 (k/o, o/e and w/t) as MOI=1 (5.10^6). After initial infection, infected cells were harvested at 0, 6, 12, 18, 24, 36, 48 and 72 hours. The harvested virus concentration was determined by the $TCID_{50}$ method that is described in part 3-10 (Figure 4.1).

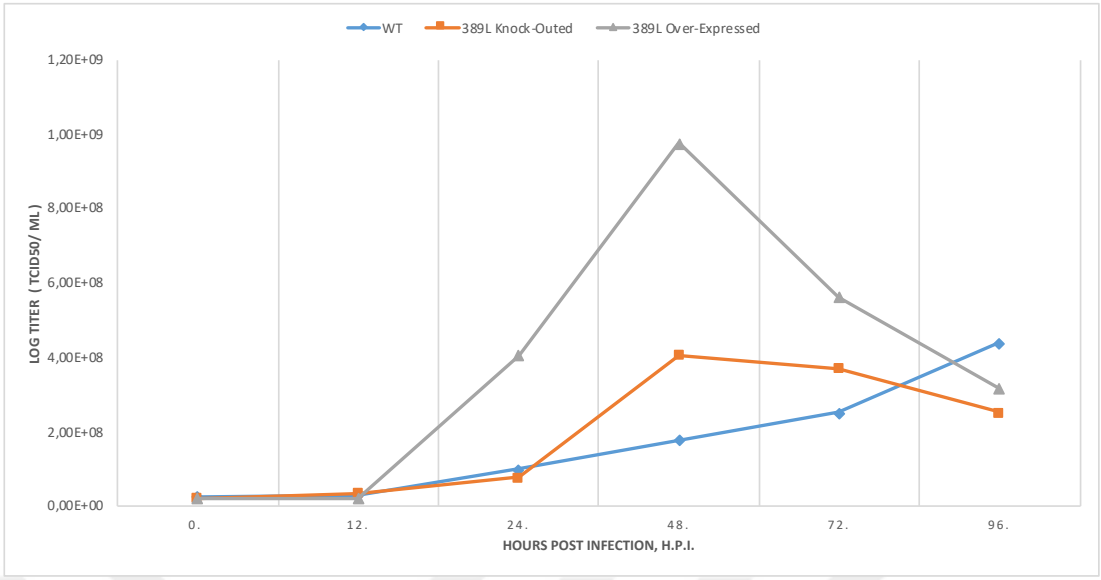

Figure 4.13 The gray arrow indicates over-expressed recombinant IIV-6, the orange arrow indicates knock-outed recombinant IIV-6 and the blue arrow indicates wild-type IIV-6,

5. DISCUSSION AND CONCLUSION

Large dsDNA viruses modulate host cell apoptosis via receptor binding, activation of protein kinase R (PKR), interaction with p53, expression of viral proteins coupled to MHC proteins on the surface of the infected cell (44,46,47). Similarly to other large dsDNA viruses, IIV-6 has a genome that can both induce and inhibit insect host cell apoptosis. In IIV-6, three genes (157L, 193R and 332L) have homology to *baculovirus iap* genes. These genes contain C-terminal RING domains, but only 193R gene contains a BIR domain. İnce et al are the first to have described an *iap* gene inhibiting apoptosis in the *iridovirus* genus. They showed that 193R gene plays a role in inhibiting apoptosis in the Sf21 and SPC-BM-36 cell lines (7) is, the study confirmed that the potential *iap* must contain BIR and RING domains, together. In addition, viruses also induce apoptosis to release their progeny to another cell line at late infection time. Paul et al were the first to show that the IIV-6 protein extract induces apoptosis in boll weevil and spruce budworm cell lines. They also determined that IIV-6 protein extract has kinase activity, whereas the mock IIV-6 protein extract from uninfected host had minimal kinase activity. For that reason, it can be assumed that kinase activity was virus-induced or the product of a virus. Additionally, they showed that heat-inactivated IIV-6 protein extract didn't induce apoptosis, and it can be suggested that one or more genes in IIV-6 are essential to inducing apoptosis (49). Moreover, in another study, Chitnis et al determined the apoptotic role of high concentration IIV-6 (400 µg/ml), UV-irradiated IIV-6 (10 µg/ml), and IIV-6 protein extract (10 µg/ml) (52). They showed that all of these IIV-6 versions induced apoptosis in 60% of the IPRI-CF-124T cell line. However, IIV-6 at a normal concentration (10 µg/ml) induced apoptosis in just 10% of the CF cell line. They also used a caspase inhibitor and showed the non-apoptosis-inducing role of all IIV-6 versions in the same experiment. This showed that caspase activation is indispensable for viral apoptosis. They also conducted an experiment to evaluate the effect of cell surface and viral entry on apoptosis. They bound UV irradiated IIV-6 to polystyrene beads, and they determined that this virus failed to induce apoptosis. For the viral entering, they used two endocytosis inhibitors: bafilomycin and ammonium chloride, and they showed

that all IIV-6 types failed to induce apoptosis, similarly. Thus, it can be suggested that viral entry is compulsory for viral-induced apoptosis. In addition to the above experiments, they also showed the apoptotic role of the JNK pathway, which is a kinase-dependent pathway. Also, it is known that activation of the JNK pathway resulting in an activation of initiator caspase Dronc induces a cascade event of caspases which causes cell apoptosis. In their experiment, they used JNK inhibitor (SP600125) in parallel with all types of IIV-6 infections, which demonstrated that apoptosis was not induced by the virus.

Protein kinases are the key partners of various viral life cycles, including replication, transcription, viral infectivity and virus uncoating (53). In apoptosis, viral infections affect the stress-related protein kinase pathway, which results in phosphorylation of the cellular transcription factor, and the induction of virus-based host apoptosis. More recently, Chitnis et al showed that a serine-threonine kinase protein of IIV-6 (389L), which is also the topic of this thesis, induces apoptosis in boll weevil cells and budworms (10). 389L belongs to Vaccinia Related Kinases (a superfamily) which, similar to other kinases, plays essential roles in chromatin condensations, apoptosis, and cellular stress (54). In addition, they determined the signature sequences of ATP binding, as well as a serine-threonine kinase in 389L gene. Moreover, they concluded that the ATP binding site is essential for the kinase and apoptotic activity of 389L. In their experiment, they generated 389L protein in a *Pichia pastoris* system. Following the generation, they evaluated the apoptotic function of the 389L protein by the TUNEL assay method. At the same time, they assigned the kinase activity of the 389L protein. This was the first study about a viral kinase inducing apoptosis in the virus-host system. Since they showed 389L inducing apoptosis at the protein level, it can be suggested that viral gene expression was not required for 389L to induce apoptosis. Furthermore, as mentioned above, IIV-6 requires endocytosis and a JNK pathway to induce apoptosis (52). Indeed, it can be claimed that 389L is involved in the JNK pathway to induce viral apoptosis.

In conclusion, various questions have been raised about viral 389L gene-host apoptotic interaction, including (i) whether this gene is involved in caspase activation, (ii)

whether other genes or metabolites could affect the apoptotic role of this gene, (iii) whether it is possible to induce IIV-6 apoptosis without 389L gene, (iv) whether over-expressing of this gene could increase apoptosis. In future studies, for the first time, recombinant IIV-6 versions will be examined to understand the questions above.

In addition to the apoptotic role of kinases, serine-threonine kinases constantly play vital roles in viral virulence. Various studies have shown that viral kinases have an essential role both in viral growth and in replication. Kovacs et al showed that the Vaccinia Virus B1 protein kinase (Figure 3.1) which is homolog to 389L gene, regulates viral replication, and affects viral growth by affecting intermediate gene expression (55). Another study showed that silencing the US3 protein kinase of Marek's disease virus (MDV) results in reduced virus growth (56). Furthermore, another study of a Vaccinia Virus B1 kinase mutant showed that US3 kinase was involved in two main stages of the virus cycle: DNA replication and the production of viral proteins (53,55,57). In this thesis, a one-step growth assay experiment showed that k/o, o/e and w/t IIV-6 viral titers clearly differ from each other. The assay showed that after 12 hours, o/e IIV-6 titer was rapidly increasing compared to w/t and k/o IIV-6. At 48 hours, o/e IIV-6 was significantly higher than 389L k/o IIV-6 (2,4 times), and w/t IIV-6 (5,5 times), while after 48 hours, although w/t IIV-6 titer had increased, k/o and o/e IIV-6 titer had decreased. In comparison to o/e IIV-6 growth, it can be speculated that k/o and w/t growth might be parallel. However, further replicative assays are required to confirm this speculation. Indeed, it can also be suggested that over-expression of 389L increases the viral titer by releasing a viral progeny cell to cell. In conclusion, further studies should be conducted to evaluate the effect of 389L on viral replication and growth.

Consequently, there are two important studies which focus on the understanding of the role of the large dsDNA viruses' kinase gene on host apoptosis and on the role of serine threonine kinase on viral replication and growth characteristic. In this thesis, o/e and k/o IIV-6 versions were shown to be crucial to the understanding of these fundamental mechanisms which may be used in anti-viral drugs for serious viral diseases such as large DNA smallpox.

6. REFERENCES

1. Wilson EO. The Future of Life. 1st Edition. Vintage; 2002.
2. Tanada Y, Kaya HK. Insect Pathology. Academic press; 2012.
3. Ignoffo CM. Development of a viral insecticide: concept to commercialization. Exp Parasitol. 1973;33(2):380–406.
4. Jenkins DA, Hunter WB, Goenaga R. Effects of Invertebrate Iridescent Virus 6 in Phyllophaga vandinei and its potential as a biocontrol delivery system. J insect Sci. 2011;11(1):44.
5. Williams T, Barbosa-Solomieu V, Chinchar VG. A decade of advances in iridovirus research. Adv Virus Res. 2005;65:173–248.
6. Henderson CW, Johnson CL, Lodhi SA, Bilimoria SL. Replication of Chilo iridescent virus in the cotton boll weevil, Anthonomus grandis, and development of an infectivity assay. Arch Virol. 2001;146(4):767–75.
7. İnce İA, Westenberg M, Vlak JM, Demirbağ Z, Nalçacıoğlu R, van Oers MM. Open reading frame 193R of Chilo iridescent virus encodes a functional inhibitor of apoptosis (IAP). Virology. 2008;376(1):124–31.
8. Hay S, Kannourakis G. A time to kill: viral manipulation of the cell death program. J Gen Virol. 2002;83(7):1547–64.
9. Jakob NJ, Müller K, Bahr U, Darai G. Analysis of the first complete DNA sequence of an invertebrate iridovirus: coding strategy of the genome of Chilo iridescent virus. Virology. 2001;286(1):182–96.
10. Chitnis NS, Paul ER, Lawrence PK, Henderson CW, Ganapathy S, Taylor PVG. A virion-associated protein kinase induces apoptosis. J Virol. 2011;JVI-05294.
11. Chen G, Ward BM, Yu EK, Chinchar VG, Robert J. Improved knockout methodology reveals that Frog Virus 3 mutants lacking either the 18K immediate-early gene or the truncated vIF2-α gene are defective for replication and growth in vivo. J Virol. 2011;JVI-05589.
12. Wang M, Yin F, Shen S, Tan Y, Deng F, Vlak JM. Partial functional rescue of Helicoverpa armigera single nucleocapsid nucleopolyhedrovirus infectivity by

replacement of F protein with GP64 from Autographa californica multicapsid nucleopolyhedrovirus. J Virol. 2010;84(21):11505–14.

13. Rucker, R. R., Thurman, W. N., & Burgett, M. Honey bee pollination markets and the internalization of reciprocal benefits. Am J Agr Econ., 2010; 94(4), 956-977.

14. Maori E, Paldi N, Shafir S, Kalev H, Tsur E, Glick E. IAPV, a bee-affecting virus associated with Colony Collapse Disorder can be silenced by dsRNA ingestion. Insect Mol Biol. 2009;18(1):55–60.

15. Inceoglu AB, Kamita SG, Hinton AC, Huang Q, Severson TF, Kang K. Recombinant baculoviruses for insect control. Pest Manag Sci. 2001;57(10):981–7.

16. Lounibos LP. Invasions by insect vectors of human disease. Annu Rev Entomol. 2002;47(1):233–66.

17. Christian PD, Possee RD. Insect Viruses. First Edition, eLS. 2008;

18. Chinchar VG, Hick P, Ince IA, Jancovich JK, Marschang R, Qin Q, ICTV virus taxonomy profile: Iridoviridae. J Gen Virol. 2017;98(5):890–1.

19. Xeros N. A second virus disease of the leatherjacket, Tipula paludosa. Nature. 1954;174(4429):562.

20. İnce İA, Özcan O, Ilter-Akulke AZ, Scully ED, Özgen A. Invertebrate Iridoviruses: A Glance over the Last Decade. Viruses, 2018, 10.4: 161.

21. King AMQ, Lefkowitz E, Adams MJ, Carstens EB. Virus taxonomy: ninth report of the International Committee on Taxonomy of Viruses. Elsevier; 2011.

22. FUKAYA M, NASU S. A. Chilo iridescent virus (CIV) from the rice stem borer, Chilo suppressalis Walker (Lepidoptera: Pyralidae). Appl Entomol Zool. 1966;1(2):69–72.

23. Yan X, Olson NH, Van Etten JL, Bergoin M, Rossmann MG, Baker TS. Structure and assembly of large lipid-containing dsDNA viruses. Nat Struct Biol. 2000;

24. Yan X, Yu Z, Zhang P, Battisti AJ, Holdaway HA, Chipman PR. The Capsid Proteins of a Large, Icosahedral dsDNA Virus. J Mol Biol. 2009;

25. Nalçacıoğlu R, Ince IA, Demirbağ Z. The biology of Chilo iridescent virus. Virol Sin. 2009;24(4):285–94.

26. Low MG. Glycosyl-phosphatidylinositol: a versatile anchor for cell surface proteins. FASEB J. 1989;3(5):1600–8.

27. Martınez G, Christian P, Marina C, Williams T. Sensitivity of Invertebrate iridescent virus 6 to organic solvents, detergents, enzymes and temperature treatment. Virus Res. 2003;91(2):249–54.

28. Marina CF, Feliciano JM, Valle J, Williams T. Effect of temperature, pH, ion concentration, and chloroform treatment on the stability of Invertebrate iridescent virus 6. J Invertebr Pathol. 2000;75(1):91–4.

29. Hernández A, Marina CF, Valle J, Williams T. Persistence of invertebrate iridescent virus 6 in tropical artificial aquatic environments. Arch Virol. 2005;150(11):2357–63.

30. Reyes A, Christian P, Valle J, Williams T. Persistence of Invertebrate iridescent virus 6 in soil. BioControl. 2004;49(4):433–40.

31. Constantino M, Christian P, Marina CF, Williams T. A comparison of techniques for detecting Invertebrate iridescent virus 6. J Virol Methods. 2001;98(2):109–18.

32. Funk CJ, Hunter WB, Achor DS. Replication of insect iridescent virus 6 in a whitefly cell line. J Invertebr Pathol. 2001;77(2):144.

33. Hunter WB, Patte CP, Sinisterra XH, Achor DS, Funk CJ, Polston JE. Discovering new insect viruses: Whitefly iridovirus (Homoptera: Aleyrodidae: Bemisia tabaci). J Invertebr Pathol. 2001;78(4):220–5.

34. Hunter WB, Lapointe SL, Sinisterra XH, Achor DS, Funk CJ. Iridovirus in the root weevil Diaprepes abbreviatus. J insect Sci. 2003;3(1).

35. Belloncik S, Petcharawan O, Couillard M, Charpentier G, Larue B, Guardado H. Development and characterization of a continuous cell line, AFKM-On-H, from hemocytes of the European corn borer Ostrinia nubilalis (Hübner)(Lepidoptera, Pyralidae). Vitr Cell Dev Biol. 2007;43(7):245–54.

36. Williams T. Invertebrate iridescent viruses. In: The insect viruses. Springer; 1998. p. 31–68.

37. Bronkhorst AW, van Rij RP. The long and short of antiviral defense: small RNA-based immunity in insects. Curr Opin Virol. 2014;7:19–28.

38. Ince IA, Özcan K, Vlak JM, van Oers MM. Temporal classification and mapping of non-polyadenylated transcripts of an invertebrate iridovirus. J Gen Virol. 2013;94(1):187–92.

39. Bronkhorst AW, van Cleef KWR, Vodovar N, İnce İA, Blanc H, Vlak JM. The DNA virus Invertebrate iridescent virus 6 is a target of the Drosophila RNAi machinery. Proc Natl Acad Sci. 2012;109(51):E3604–13.

40. Ince IA, Boeren S, van Oers MM, Vlak JM. Temporal proteomic analysis and label-free quantification of viral proteins of an invertebrate iridovirus. J Gen Virol. 2015;96(1):196–205.

41. Goorha R. Frog virus 3 DNA replication occurs in two stages. J Virol. 1982;43(2):519–28.

42. Barray S, Devauchelle G. Protein synthesis in cells infected by Chilo iridiscent virus: evidence for temporal control of three classes of induced polypeptides. Elsevier; 1987. p. 253–61.

43. D'Costa SM, Yao H, Bilimoria SL. Transcription and temporal cascade in Chilo iridescent virus infected cells. Arch Virol. 2001;146(11):2165–78.

44. D'Costa SM, Yao HJ, Bilimoria SL. Transcriptional mapping in Chilo iridescent virus infections. Arch Virol. 2004;149(4):723–42.

45. Elmore S. Apoptosis: a review of programmed cell death. Toxicol Pathol. 2007;35(4):495–516.

46. Hengartner MO. The biochemistry of apoptosis. Nature. 2000;407(6805):770.

47. Abraham MC, Shaham S. Death without caspases, caspases without death. Trends Cell Biol. 2004;14(4):184–93.

48. Thomson BJ. Viruses and apoptosis. Int J Exp Pathol. 2001;82(2):65–76.

49. Paul ER, Chitnis NS, Henderson CW, Kaul RJ, D'Costa SM, Bilimoria SL. Induction of apoptosis by iridovirus virion protein extract. Arch Virol. 2007;152(7):1353–64.

50. Hall, T., Biosciences, I., & Carlsbad, C. (2011). BioEdit: an important software for molecular biology. GERF Bull Biosci, 2(1), 60-61.

51. Hierholzer JC, Killington RA. Virus isolation and quantitation. Virology methods manual. Elsevier; 1996. p. 25–46.

52. Chitnis NS, D'Costa SM, Paul ER, Bilimoria SL. Modulation of iridovirus-induced apoptosis by endocytosis, early expression, JNK, and apical caspase. Virology. 2008;370(2):333–42.

53. Jacob T, Van den Broeke C, Favoreel HW. Viral serine/threonine protein kinases. J Virol. 2011;85(3):1158–73.

54. Klerkx EP, Lazo PA, Askjaer P. Emerging biological functions of the vaccinia-related kinase (VRK) family. Histol Histopathol. 2009;24(6):749–59.

55. Kovacs GR, Vasilakis N, Moss B. Regulation of viral intermediate gene expression by the vaccinia virus B1 protein kinase. J Virol. 2001;75(9):4048–55.

56. Schumacher D, McKinney C, Kaufer BB, Osterrieder N. Enzymatically inactive US3 protein kinase of Marek's disease virus (MDV) is capable of depolymerizing F-actin but results in accumulation of virions in perinuclear invaginations and reduced virus growth. Virology. 2008;375(1):37–47.

57. Rempel RE, Anderson MK, Evans E, Traktman P. Temperature-sensitive vaccinia virus mutants identify a gene with an essential role in viral replication. J Virol. 1990;64(2):574–83.

7. CURRICULUM VITAE

Personal Information

Name	Ömer Faruk	**Surname**	Taştan
Birth of place	Ağrı	**Date of birth**	01.06.1993
Nationality	T.C.	**Telephone number**	+905077966292
E-mail	oftastan@gmail.com		

Educational Level		
	Institution Name	**Graduate Year**
Master	Mehmet Ali Aydınlar Acibadem University	2019
Undergraduate	Istanbul University	2016
High-School	Alpaslan Anadolu Öğretmen Lisesi	2011

Work Experience

	Position	**Enterprise**	**Duration**
1.	WWF	Face to Face Fundraiser	2014-2015
2.	Micro S Biyoteknoloji A.Ş.	Founder	2017-

Foreign Languages	**Reading***	**Speaking***	**Writing***
English	Very good	Good	Good

Foreign Languages Exams•

YÖK-DİL	**UDS**	**IELTS**	**TOEFL IBT**	**TOEFL PBT**	**TOEFL CBT**	**FCE**	**CAE**	**CPE**
73,75								

	Quantitative	**Equally Weighted**	**Verbal**
ALES Exam	87,39	87,52	74,24

Projects				
	Granted Program	**Active Years**	**Position**	**Project Name**
1.	TUBITAK 1512	2017-2018	Coordinator	Bal arılarının Sağlığının Korunması İçin Doğal Probiyotik Kokteyller
2.	TUBITAK 1001	2016-2017	Scholarship student	Gribal Enfeksiyonlarda Epigenetik Kontrol Mekanizmaların Araştırılması

Presentations & Awards			
	Organization	**Presentation Type**	**Title of the Presentation**

1.	Ege İhracatçılar Birliği Gıda Arge Proje Pazarı, İzmir	Poster	Domates Yetiştiriciliğinde Hormonlar Yerine Yeni Doğa Dostu Yöntem: Bitki Büyüme Teşvik Edici Bakteri (Plant Growth Promoting Bacteria)
2.	Third FAO/IAEA International Conference on Area-wide Management of Insect Pests, Vienna	Poster	Exploring the biocontrol agents for Ricania simulans (Walker, 1851) and its microbiota,
3.	Materials Today Communications	Publication	Insecticide-releasing LLDPE films as greenhouse cover materials